

The Effect of Microwave Irradiation on the Physicochemical Properties of Pyrite

Jabun Nahar Mita

Department of Mining and Materials Engineering
McGill University
Montreal, Quebec, Canada
April 2018

A Thesis Submitted to the Faculty of Graduate studies and Research in Partial Fulfilment of the Requirements for the Degree of Master of Engineering

©Jabun Nahar Mita, 2018

Acknowledgements

This thesis was an academic and personal journey that I was capable of undergoing due to the support of my supervisor, research group, family and friends.

First, I want to thank my supervisor, Prof. Kristian E. Waters, for his generosity, understanding, and advice. Without his consistent and unwavering support, I would not have been able to complete this project.

I want to thank the mineral processing group for their advice and training. I would like to thank Ray Langlois for helping with the preparation of my experimentations, training, and being a friend. I want to thank Adam Jordens for taking my samples to Birmingham to do the VSM experiments. I want to thank Christopher Marion for helping me with the electroacoustic zeta potential experiments. I want to especially thank Eileen Espiritu and Gilberto Rodrigues da Silva for their many advice throughout this journey.

I also want to thank Florence Paray for the SEM training, Sriraman Rajagopalan for XRD training, Lihong Shang for XPS training, Pejman Nekoovaght for the use of the microwaves, and Monique Riendeau for BET and PSA training.

I want to thank all the sponsors for their financial support: McGill University, NSERC, Vale, XPS Consulting & Testwork Services, Teck, Shell, SGS, Corem, Flottec, and Barrick.

I want to thank my parents, Enamul Haque and Shoheli Begum, for their unconditional love and support in everything that I take on. I want to thank my siblings, Naomi Haque and Nabil Haque. I want to thank my in laws, Rezaul Chaowdhury, Nahid Chowdhury, and Rakhee Chowdhury for their patience, love, and support in this journey.

Finally, I want to thank my husband, Rajib Chowdhury, for his patience, love, guidance, and for continually challenging me to my limits so that I may grow. I also want to thank him for his time, advice and his help. Without his love, none of this would be possible. I also want to thank Allah who has generously blessed me with all these wonderful people to give me the strength required to complete this thesis.

Abstract

Comminution is an energy intensive process which consumes 30% to 70% of the energy used in mining. In the last few decades, thermal treatment of minerals has been researched with the goal of reducing the energy required in comminution. Microwave radiation has proven to reduce the energy required in this stage.

It has been shown that microwave radiation improves the grindability and liberation of minerals due to the differential dielectric heating which leads to intergranular fractures. In addition, microwave radiation has been found to cause phase transformations at the grains of the minerals. This thesis investigates the effect of microwave irradiation on the downstream separation processes, namely flotation. The latter can help assess whether the positive effects the microwave irradiation has in the comminution stage will be detrimental or useful in the separation of valuable minerals from gangue minerals downstream.

This thesis looks at the effect that microwave pre-treatment has on a common sulfide mineral: pyrite. Pyrite is typically a gangue (non-valuable) mineral that should be depressed during the flotation process; however, it reacts with reagents during flotation and can float with the valuable mineral. When exposed to microwave radiation, phase transformation is observed on the surface of the mineral which can alter the mineral's surface chemistry, surface charge, magnetic susceptibility, and degree of hydrophobicity.

Weakly paramagnetic pyrite became ferromagnetic after exposure to microwave treatment. It was also found that pyrite recovery in the presence of PAX decreased from pH 3-11 after exposure to microwave radiation.

Résumé

Le broyage est un processus qui consomme 30% à 70% de l'énergie utilisée dans l'exploitation minière. Au cours des dernières décennies, le traitement thermique des minéraux a été étudié dans le but de réduire l'énergie nécessaire au broyage. L'irradiation par micro-onde peut réduire l'énergie requis dans cette étape.

Il a été démontré que le rayonnement micro-ondes améliore le meulage et la libération de minéraux en raison du chauffage diélectrique différentiel qui cause des fractures intergranulaires. De plus, on a constaté que le rayonnement des micro-ondes suscite des transformations de phase sur les grains des minéraux. Cette thèse examine l'effet de l'irradiation des micro-ondes sur les processus de séparation subséquent, principalement la flottation. Cette compréhension peut aider à évaluer si les effets positifs qu'il a eu dans la phase de broyage seront préjudiciables ou utiles à la séparation des minéraux précieux des minéraux non précieux.

Cette thèse examine l'effet que le prétraitement des micro-ondes a sur un minerai de sulfure commun: la pyrite. La pyrite est généralement un minéral non valable qui devrait être déprimé pendant le processus de flottation ; cependant, elle réagit avec les réactifs pendant la flottation et peut flotter avec le minéral précieux. Lorsqu'elle est exposée au rayonnement micro-ondes, une transformation de phase est observée à la surface du minéral qui peut altérer la chimie sur la surface du minéral, la charge de surface, la susceptibilité magnétique et le degré d'hydrophobicité.

La pyrite qui était faiblement paramagnétique est devenue ferromagnétique après exposition au traitement par rayonnement micro-ondes. On a également constaté que la récupération de pyrite en présence de PAX a diminué de pH 3-11 après exposition au rayonnement hyperfréquence.

Contents

Acknowledgements.....	i
Abstract.....	iii
Résumé.....	v
Contents	vii
List of Figures.....	xi
List of Tables	xiv
1 Introduction.....	1
1.1 Introduction	1
1.2 Objective	4
1.3 Structure of the thesis.....	5
2 Mineral Processing.....	7
2.1 Introduction	7
2.2 Comminution.....	8
2.3 Separation Techniques	9
2.3.1 Gravity Separation	9
2.3.2 Froth Flotation	10
2.3.3 Magnetic Separation	13

2.3.4	Electrostatic Separation	14
2.4	Measures of Separation	15
3	Microwave Treatment of Minerals	16
3.1	Thermally Assisted Liberation (TAL).....	16
3.2	Microwaves	18
3.2.1	Factors Affecting Dielectric Heating	20
3.3	Use of Microwaves in Mineral Processing	23
4	Physicochemical Properties of Minerals.....	26
4.1	Surface Chemistry	26
4.1.1	Zeta Potential	27
4.2	Magnetism.....	30
4.2.1	Magnetic Moment.....	31
4.2.2	Magnetisation.....	31
4.2.3	Magnetic Susceptibility	33
4.2.4	Vibrating Sample Magnetometer (VSM).....	33
5	Methodology	35
5.1	Introduction	35
5.2	Materials.....	35
5.2.1	Pyrite.....	35
5.2.2	Potassium Amyl Xanthate (Collector).....	36

5.3	Sample Preparation	38
5.3.1	Mineral Purification	38
5.4	Microwave Treatment	39
5.5	Surface Characterization techniques	39
5.5.1	X-Ray Diffraction (XRD).....	39
5.5.2	X-Ray Photon Spectrometer (XPS)	39
5.5.3	Scanning Electron Microscope (SEM)	40
5.5.4	Vibrating Sample Magnetometer (VSM).....	40
5.5.5	Zeta Potential	41
5.6	Microflotation.....	42
5.6.1	Single Mineral.....	42
6	Results.....	44
6.1	Temperature Analysis	44
6.2	Surface Characterization	46
6.2.1	XRD	46
6.2.2	XPS	47
6.2.3	SEM	50
6.3	Magnetic Properties.....	52
6.4	Zeta Potential.....	55
6.5	Microflotation.....	57

7	Conclusions and Future Work	61
7.1	Conclusions	61
7.2	Future work	62
8	References.....	64

List of Figures

Figure 1.1 Particle liberation schematic.....	1
Figure 1.2 Improved liberation of chalcopyrite after exposure to microwave radiation (Kobusheshe, 2010)	2
Figure 1.3 Decreased flotation recovery after exposure to microwave radiation (Vorster, 2001) .	3
Figure 1.4 Increased magnetic recovery after exposure to microwave radiation (Waters, 2007) ..	4
Figure 2.1 Simplified block flow diagram for mineral processing with the comminution steps highlighted in blue. Separation of minerals can be achieved through gravity separation, electrostatic separation, magnetic separation, or froth flotation (to name a few methods)	8
Figure 2.2 Schematic of froth flotation process for mineral separation (Wills and Finch, 2016)	11
Figure 2.3 Schematic of the three interfacial energies and the contact angle between mineral surface and air bubble in flotation (Wills and Finch, 2016)	11
Figure 2.4 Operational schematic of an HTR separator (Wills and Finch, 2016)	14
Figure 2.5 Typical grade-recovery curve.....	16
Figure 3.1 Schematic of two types of fractures a) intergranular fracture b) transgranular fracture	18
Figure 3.2 Simplified Microwave Heating System.....	19
Figure 3.3 Variation of dielectric constant with temperature for selected minerals (Kobusheshe, 2010)	22
Figure 3.4 Variation of loss factor with temperature for selected minerals (Kobusheshe, 2010)	23
Figure 4.1 The change in free energy as a function of particle separation (Trefalt and Borkovec, 2014)	27

Figure 4.2 Diffuse double layer of a mineral particle with the point of measurement of zeta potential.....	28
Figure 4.3 (a) Flotation response of a mineral to two different collectors - anionic and cationic - as a function of pH (b) surface charge as a function of pH. 1×10^{-4} M NaCl is the background electrolyte to keep a constant ionic strength. (Wills and Finch, 2016).....	29
Figure 4.4 Magnetization of different magnetic materials.....	32
Figure 4.5 Magnetic susceptibility versus field strength for a diamagnetic, paramagnetic, and ferromagnetic material	33
Figure 4.6 Schematic of a vibrating sample magnetometer.....	34
Figure 5.1 Experimental Steps.....	35
Figure 5.2 Schematic of the Modified Hallimond Tube (a) the process (b) parts	42
Figure 6.1 The effect of particle size on the bulk temperature of pyrite sample treated in a 3kW microwave oven for 10s.....	45
Figure 6.2 The effect of power level on the bulk temperature of -425+38 micrometer pyrite sample treated for 15s.	46
Figure 6.3 The effect of exposure time on the bulk temperature of -425+38 micrometer pyrite sample treated in a 3kW microwave oven.	46
Figure 6.4 Iron spectrum of microwave treated pyrite and untreated pyrite from XPS showing the iron phases present.....	48
Figure 6.5 Sulfur spectrum of microwave treated pyrite and untreated pyrite from XPS showing the different sulfur phases present	49
Figure 6.6 Oxygen spectrum of microwave treated pyrite and untreated pyrite from XPS showing the oxygen phases present.....	49

Figure 6.7 Left - SEM image of pyrite exposed to microwave radiation for 30s at a power level of 3 kW. Right - Optical microscope image of the cross section of pyrite grains after exposure to microwave radiation for 30s at a power level of 3 kW.....	50
Figure 6.8 SEM image of a partial decomposition of a pyrite grain after ore was exposed to microwave radiation (Vorster, 2001).....	51
Figure 6.9 SEM image with EDS with the phase maps of a pyrite sample exposed to microwave radiation for 10s at a power level of 3 kW.....	52
Figure 6.10 VSM results for -425+212 μm pyrite exposed to microwave radiation for 10s at a 3kW power level.....	54
Figure 6.11 VSM results for -212+75 μm pyrite sample exposed to microwave radiation for 10s at 3 kW power level	54
Figure 6.12 VSM results for -75+38 μm pyrite sample exposed to microwave radiation for 10s at 3kW power level.....	54
Figure 6.13 Zeta potential of collectorless untreated pyrite and pyrite treated in a 3 kW microwave oven for 15s and 30s with a 95% confidence interval.	57
Figure 6.14 Zeta potential using PAX as a collector of untreated pyrite and pyrite treated in a 3 kW microwave oven for 15s and 30s with a 95% confidence interval.....	57
Figure 6.15 Pyrite recovery as a function of conditioning time with a 95% confidence interval	58
Figure 6.16 Pyrite recovery as function of PAX concentration with a 95% confidence interval.	59
Figure 6.17 Flotation recovery without collector for untreated pyrite and pyrite treated for 15s and 30s in a 3kW microwave as a function of pH with a 95% confidence interval	59
Figure 6.18 Flotation recovery with PAX for untreated pyrite and pyrite treated for 15s and 30s in a 3kW microwave as a function of pH with a 95% confidence interval	60

List of Tables

Table 3-1 Interaction of Microwave Radiation with Different Materials.....	20
Table 6-1: Untreated and treated pyrite ferromagnetic components using literature data.....	53

1 Introduction

1.1 Introduction

Mineral processing is the processing of ores to yield concentrated valuable products through two primary stages: comminution and concentration. In comminution, the mineral goes through the crushing and grinding stages to sufficiently decrease the particle size to achieve the liberation of the valuable mineral. In the concentration stage, the valuable mineral is separated and concentrated from the non-valuable (gangue) mineral. The objective of mineral processing is to separate the valuable mineral from the gangue mineral (2003).

Liberation of valuable minerals from non-valuable mineral is the essential goal of comminution. As shown in Figure 1.1, this is achieved by fracturing the ore to produce smaller particles that are either completely liberated in the form of valuable minerals and non-valuable minerals (gangue) or middlings, which are partially liberated particles. This step enables the maximization of the liberation necessary to send the product to the downstream processes.

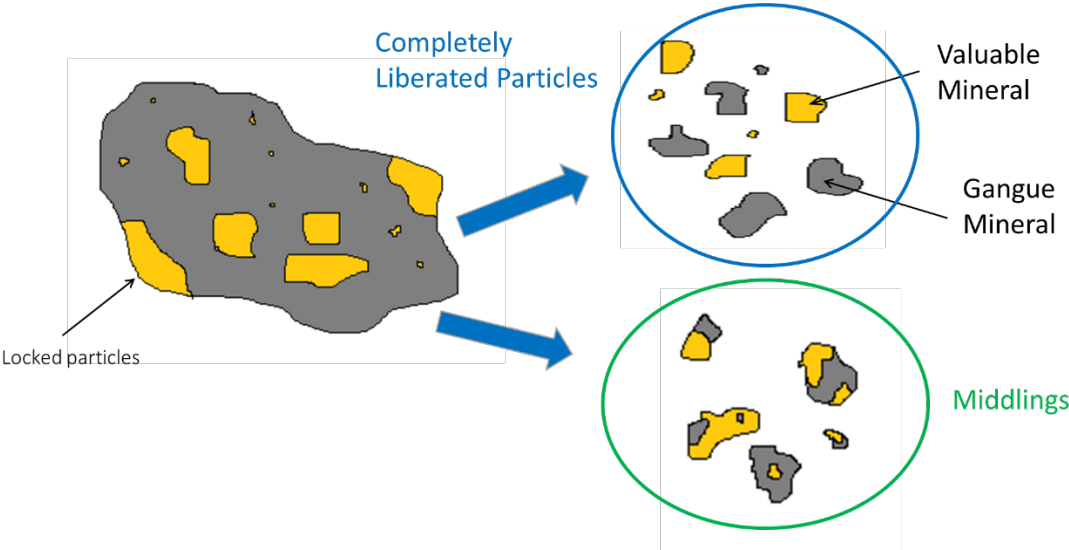


Figure 1.1 Particle liberation schematic

Conventional comminution techniques have a high energy usage, consuming about 30-70% of the energy used in mining (Nadolski et al., 2014; Radziszewski, 2013). The bulk of the energy is used in fine grinding, which is the last stage in the comminution circuit (Napier-Munn, 2015). Of the 70%, only 1-2% of the energy is used for breakage (Fuerstenau and Abouzeid, 2002); consequently, this process is very inefficient.

Literature suggests various ways to pre-treat the ore to facilitate the grinding process. Some of these include: hydraulic, ultrasonic, electrical, and microwave irradiation (Amankwah and Ofori-Sarpong, 2011; Andres, 2010; Andres, 1977; Andriese et al., 2011; Gaete-Garretón et al., 2000; Leonelli and Mason, 2010; Parekh et al., 1984; Shi et al., 2013; Teipel et al., 2004; Wang et al., 2012; Yerkovic et al., 1993). This thesis focuses on the microwave pre-treatment process.

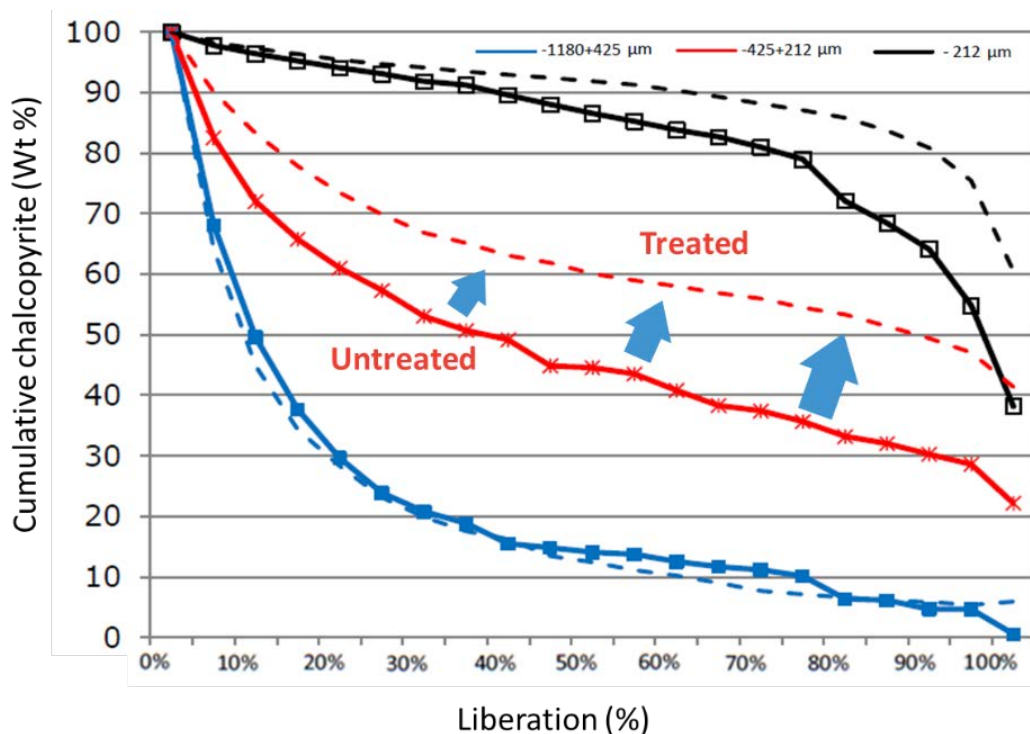


Figure 1.2 Improved liberation of chalcopyrite after exposure to microwave radiation (Kobusheshe, 2010)

Different minerals heat differently when exposed to microwave radiation. The heating causes thermal stress at the grain boundaries thus fracturing the material (Fitzgibbon and Veasey, 1990). Due to this, the grindability and liberation can be improved. Figure 1.2 demonstrates that there is an increase in liberation after chalcopyrite has been exposed to microwave radiation (Kobusheshe, 2010). However, phase transformation has also been observed at the grain boundaries of minerals. This change can have effects on downstream processes such as magnetic separation and froth flotation as seen in Figure 1.3 and Figure 1.4 (Vorster, 2001; Waters et al., 2007). The flotation recovery decreased after exposure to microwave, whereas the magnetic

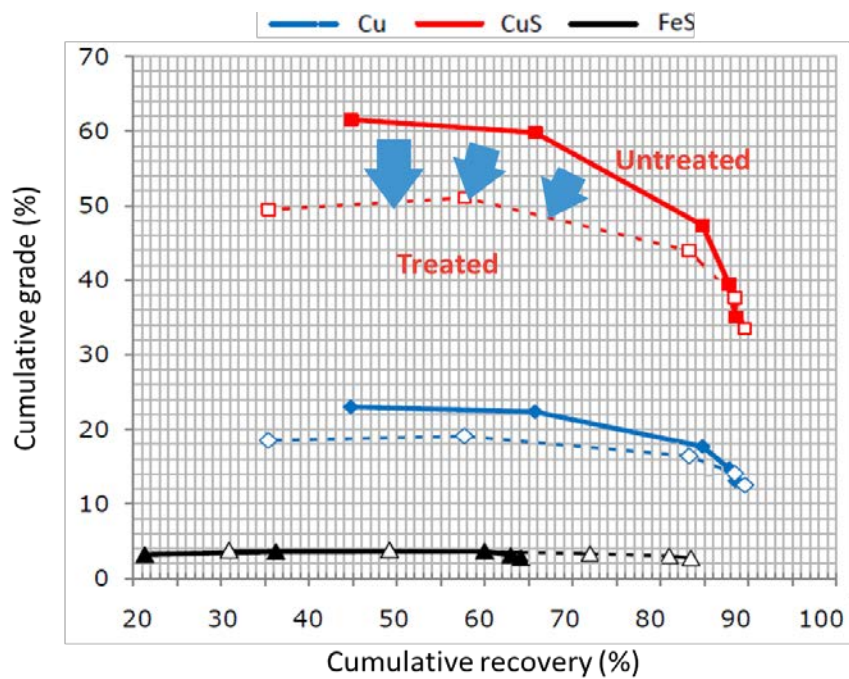


Figure 1.3 Decreased flotation recovery after exposure to microwave radiation (Vorster, 2001) recovery increased suggesting a change had occurred on the surface of the mineral.

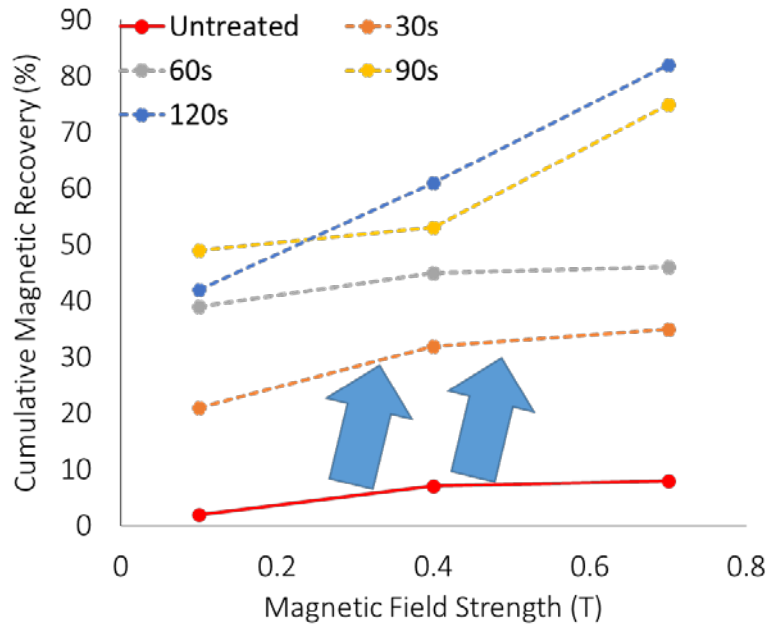


Figure 1.4 Increased magnetic recovery after exposure to microwave radiation (Waters, 2007)

1.2 Objective

The goal of this thesis was to understand the effect on the surface characteristic of pyrite after pre-treating pyrite with microwave radiation. The following was investigated:

- Temperature analysis was done to understand the effect of particle size, microwave power level, and microwave radiation exposure time
- The surface speciation was examined using XPS to see if there were any formation of new phases
- The magnetization was inspected using a vibrating sample magnetometer (VSM) to see understand the changes in the magnetic properties
- The surface charge by measuring the zeta-potential since this could have an affect on floatability
- Hydrophobicity was interpolated by conducting microflotation experiments

1.3 Structure of the thesis

This thesis consists of 7 chapters. The outline of the individual chapters is as follows:

Chapter 1: Introduction

Information on the problems with the comminution process is presented. This is important to understand the reasons behind microwave radiation is being investigated. This leads to the research motivations and objectives. Followed by an overview of the thesis structure.

Chapter 2: Mineral Processing

Introduction to mineral processing. The goal of comminution; separation techniques used in mineral processing and how to measure the efficacy of these techniques.

Chapter 3: Microwave

Introduction into thermally assisted liberation. What microwave radiation consists of and the parameters that affect microwave heating of minerals. Demonstrates how microwave radiation can be used in mineral processing.

Chapter 4: Physicochemical Properties of Minerals

Background on the physicochemical techniques that were used in the project to better understand the results presented.

Chapter 5: Methodology

Background on properties of pyrite and PAX are presented in the materials. A detailed description of the experimental procedures used throughout this research.

Chapter 6: Results

Results for the temperature analysis, surface characterization, magnetic properties, and microflotation were presented and discussed.

Chapter 7: Conclusion

The major conclusions of the thesis and suggestion for further research are presented in this chapter.

2 Mineral Processing

2.1 Introduction

Minerals and the products obtained from minerals have contributed to the industrialization of society and the advancements in technology that humans have become accustomed to. Coal is still one of the world's largest energy source. Copper is used in electric wires, switches, heating, roofing, pharmaceutical machinery, and building constructions. Gold is used in dentistry, medicine, jewelry, electronic instruments, and in the electro-plating industry. Mica is used in electronic insulators, paint, welding rods, and as a dusting agent. Quartz is used in pressure gauges, resonators, heat-ray lamps, and glass. These are only a few examples of the use of minerals in everyday life. Consequently, the world could not run without minerals.

It is important to distinguish the difference between minerals, rocks and ores. Minerals are chemical compounds that are normally crystalline and form due to geological processes (Nickel, 1995). Rocks are compounds of minerals (Metso et al., 2015). Ores are rocks at high enough concentration of certain minerals that it can be extracted economically and legally. The ore can contain valuable minerals or non-valuable minerals (gangue). The extraction of minerals using physicochemical processes is known as mineral processing. It is the step that follows mining and prepares the ore for extraction of the valuable metal or to produce a commercial product.

The objective of mineral processing is to separate the valuable mineral from the non-valuable mineral while producing maximum value from the raw material. This is achieved primarily in two stages: comminution and concentration (separation). In the comminution stage, the particle size is reduced to achieve liberation through crushing and grinding processes. In the

concentration stage, the valuable mineral is separated from the gangue mineral. This process is shown in Figure 2.1.

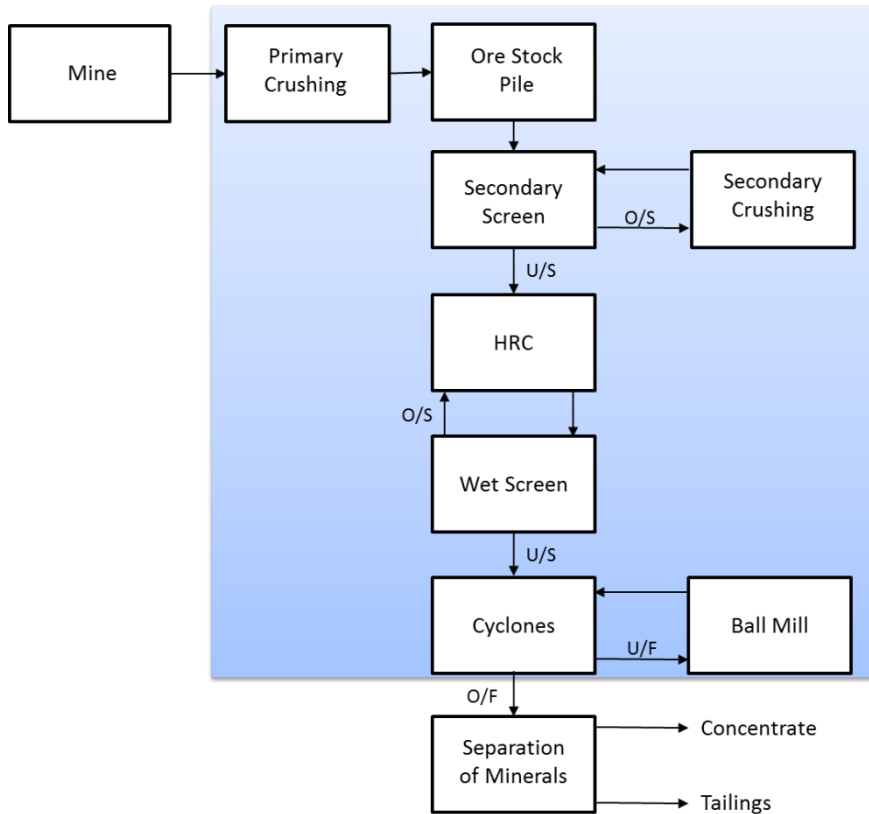


Figure 2.1 Simplified block flow diagram for mineral processing with the comminution steps highlighted in blue. Separation of minerals can be achieved through gravity separation, electrostatic separation, magnetic separation, or froth flotation (to name a few methods)

2.2 Comminution

Comminution refers to the mechanical breakage of rocks into smaller particles (Napier-Munn, 1999; Vorster, 2001). The objective of this step is to break the ore into smaller sizes to “unlock” or “liberate” the valuable mineral from the gangue mineral and to increase the efficiency of the

concentration stage. Comminution includes crushing units, tumbling mills, stirred mills, grinding units, as well as sizing processes (Napier-Munn, 1999; Vorster, 2001). Crushing reduces the particle size of the run-of-mine (ROM) ore in several stages to enable grinding to be carried out (Wills and Finch, 2016). Grinding is the most important operation for the liberation of the valuable mineral (Wills, 1990).

Conventional comminution techniques have a high energy usage. It consumes about 30-70% of the energy used in mining (Nadolski et al., 2014; Radziszewski, 2013). The bulk of the energy is used in fine grinding; which is the last stage in the comminution circuit (Napier-Munn, 2015). Of this, only 1-2% of the energy is used for the breakage (Fuerstenau and Abouzeid, 2002; Vorster, 2001). Thus, making comminution an energy inefficient process. Consequently, a reduction in the energy requirement for the milling process would lead to a great decrease in the operating cost. Thermally assisted liberation (TAL) is a possible solution to reduce the cost of comminution and the energy usage (Wills et al., 1987). This will be discussed in greater detail in Chapter 3.

2.3 Separation Techniques

2.3.1 Gravity Separation

Gravity separation utilizes the differences in the specific gravity of minerals to achieve separation. The particles respond mainly to the force of gravity, buoyancy, and fluid drag (Jordens, 2016; Wills and Finch, 2016). For the separation to be effective, there must be a pronounced difference in the density of the minerals being separated. The concentration criterion ($\Delta\rho$) can gauge the possible separation that can be obtained:

$$\Delta\rho = \frac{\rho_h - \rho_\ell}{\rho_l - \rho_\ell} \quad (1)$$

Where ρ_h is the density of the heavy mineral, ρ_l is the density of the light mineral, and ρ_f is the density of the fluid medium (Wills and Finch, 2016). In general, if the concentration criterion is greater than 2.5, a good separation can be achieved (Jordens, 2016). In addition to the specific gravity of the mineral, the particle size can also affect the efficiency of the separation. The gravitational force will have a greater affect on larger particles; whereas, smaller particles will be dominated more by surface friction (Anon, 1980; Metso et al., 2015; Minerals, 2004). Particles greater than 500 μm will be ruled by Newton's law and particles smaller than 50 μm will be ruled by Stoke's law (Jordens, 2016).

2.3.2 Froth Flotation

Flotation is a separation process that exploits the differences in the degrees of hydrophobicity, or water repulsion, of mineral particles (Waters, 2007; Wills and Finch, 2016). Flotation is a three-phase system of solid, water, and air phases. The air bubbles pass through a pulp of mineral ore and water. Chemical variables control the hydrophilicity of the particle. Physical variables are results of the properties of the ore – particle size, composition, and liberation – and machine-derived such as air rate and bubble size. Hydrophobic particles can attach to the air bubbles and float to the surface; whereas hydrophilic particles will remain in the pulp solution as shown in Figure 2.2 (Wencheng and Jianguo Yan, 2013).

One of the important variables in flotation practice is the pH of the solution because the collection of valuable minerals varies over a pH range (Fan and Rowson, 2002; Henda et al., 2005). Since froth flotation is a physicochemical process, it depends on complex phenomena that occur at the interface between mineral surfaces and air bubbles (Cheng et al., 2004). Therefore, any changes to the surface could induce considerable changes in the flotation performance.

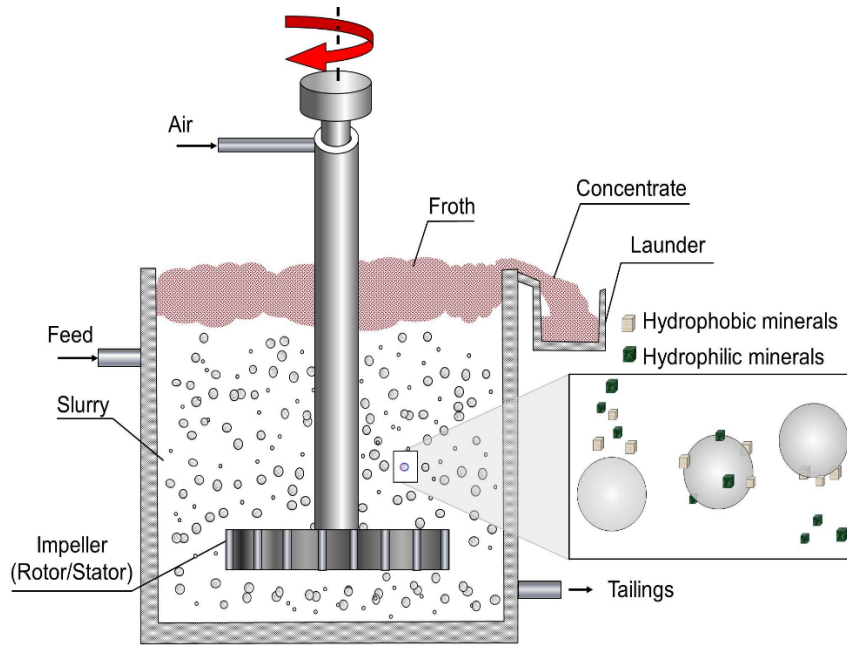


Figure 2.2 Schematic of froth flotation process for mineral separation (Wills and Finch, 2016)

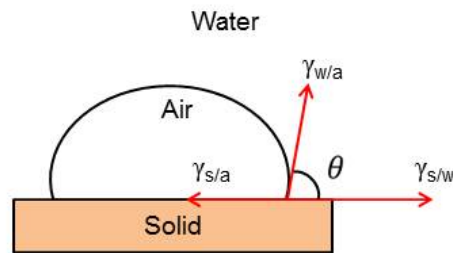


Figure 2.3 Schematic of the three interfacial energies and the contact angle between mineral surface and air bubble in flotation (Wills and Finch, 2016)

2.3.2.1 Hydrophobicity

The interaction between a solid mineral particle and an air bubble can be understood through the interfacial energies of each of the surfaces: solid-air ($\gamma_{s/a}$), water-air ($\gamma_{w/a}$), and solid-water ($\gamma_{s/w}$) as shown in Figure 2.3.

At equilibrium, the tensile force between the mineral surface and the bubble surface can be expressed as Equation 2, where θ is the contact angle between the mineral surface and the bubble. The contact angle indicates the extent of hydrophobicity of the mineral. For instance, mineral surfaces that are more hydrophobic will have a higher contact angle with water and a greater work of adhesion (Wills and Finch, 2016). Work of adhesion, $W_{s/a}$, is the force required to break the particle-bubble interface and is stated in Equation 3. When the two equations are combined, Equation 4 is obtained.

$$\gamma_{s/a} = \gamma_{s/w} + \gamma_{w/a} \cos \theta \quad (2)$$

$$W_{s/a} = \gamma_{w/a} + \gamma_{s/w} - \gamma_{s/a} \quad (3)$$

$$W_{s/a} = \gamma_{w/a}(1 - \cos \theta) \quad (4)$$

2.3.2.2 Flotation Kinetics

The first order rate equation is often used to describe the recovery of a given mineral in flotation as a function of time (Ahmed and Jameson, 1989; Feteris et al., 1987; Polat and Chander, 2000), as shown in Equation 5.

$$R = R_{max}(1 - e^{-kt}) \quad (5)$$

Where t is flotation time (min), k is the flotation rate constant (min^{-1}) and R_{max} is the maximum recovery achievable at $t=\infty$. Comparison of flotation rate constants for different minerals is commonly used as a predictor for the possibility of a separation of two floatable components based on the kinetic rate of flotation recovery.

2.3.2.3 *Reagents*

Reagents are often used in flotation processes to alter the hydrophobic nature of the mineral surfaces. The addition of the reagent can either:

- 1) Increase the hydrophobic nature of the surface by adsorbing to the surface of the particle which is achieved through the addition of collectors.
- 2) Increase the hydrophilicity on the particle surface which is achieved through the addition of depressants

Frothers are surfactants of low solubility and surface tension that promote the stability of the froth phase and preserve the bubble size in flotation. They should not react with collectors or act as a collector (Waters, 2007).

Many valuable mineral are naturally hydrophilic; as such, collectors are added to chemically alter the surface of the minerals by adsorbing to the selected mineral surface and partially covering it with a thin film that is water repellent. This modifies the mineral surface to become hydrophobic (Muzenda and Afolabi, 2010; Waters, 2007).

Depressants prevent the flotation of certain minerals through one or a combination of the following mechanisms: adsorption of hydrophilic species, blocking of collector adsorption sites, or removal (desorption) of activating species, and/or removal of hydrophobic sites (Nagaraj and Ravishankar, 2007).

2.3.3 *Magnetic Separation*

Different minerals have different magnetic characteristics. They can be either ferromagnetic, paramagnetic or diamagnetic. This property can be used to separate minerals using different magnetic field intensities.

Magnetic separators are generally classified as either low intensity, high intensity machines, or high gradient. Low intensity separators are used to treat ferromagnetic materials and some paramagnetic materials. This is because ferromagnetic materials have a high susceptibility at low applied field strength ($<0.3T$) (Minniberger et al., 2014; Murariu and Svoboda, 2003). High intensity separators can effectively recover weakly paramagnetic minerals using an applied field strength greater than $2T$ (Svoboda, 1994). High intensity separation can treat a dry or slurry feed (Wills and Finch, 2016). High field gradient separators are used to separate paramagnetic minerals that have a low magnetic susceptibility and/or fine size (Svoboda, 2001).

2.3.4 Electrostatic Separation

Electrostatic separation utilizes the difference in mineral conductivity, contact potential, or dielectric constant to separate minerals (Eskibalci and Ozkan, 2012). This method has limited applications in practice because of the required processing conditions — mainly that the feed needs to be perfectly dry. The most common electrostatic separator is the high-tension roll (HTR) separator as shown in Figure 2.4. A dry feed of particles is fed to the top of a rotating earthed roll. The particles then pass through a spray discharge ionizing electrode where the mineral acquires a surface charge. Once past the ionizing electrode's field, strongly conductive minerals will quickly lose this charge to the earthed roll and will be thrown off the roll while weaker conducting minerals will maintain this charge and remain pinned to the roll. The weakly

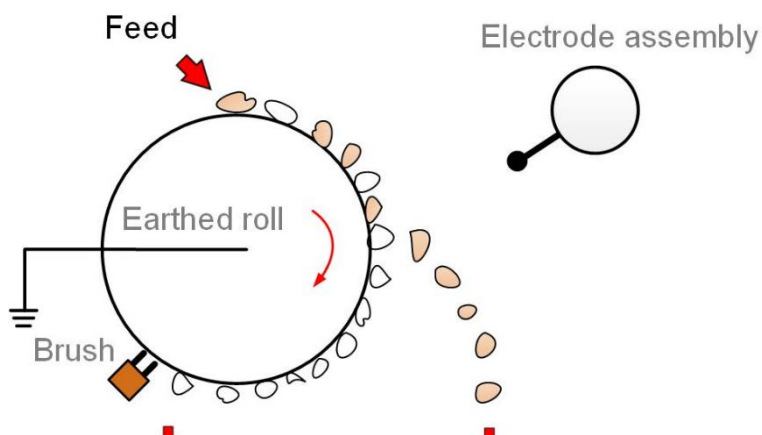


Figure 2.4 Operational schematic of an HTR separator (Wills and Finch, 2016)

conducting minerals are then removed from the roll using a brush (Jordens, 2016; Kelly and Spottiswood, 1989a, b; Wills and Finch, 2016).

2.4 Measures of Separation

It is not possible to have complete separation of the valuable minerals from the gangue minerals; however, grade and recovery can be used as measures of the separation performance or effectiveness. This measure is commonly applied to metals and not minerals. The recovery compares the quantity of valuable metal in the product to the valuable metal in the feed. The aim is to have as high of a recovery as is economically and technologically possible. Grade refers to the purity of the concentrate stream. It is the percent by mass of the metal in solid and it is dependent on the chemical composition of the metal.

In general, as grade increases, recovery decreases Figure 2.5 shows a typical grade-recovery curve. The trade-off is dependent on economic parameters. The optimum grade and recovery is primarily dependent on the plant design and operation, metal price, and smelter contracts. The optimum point is where the net return is maximized.

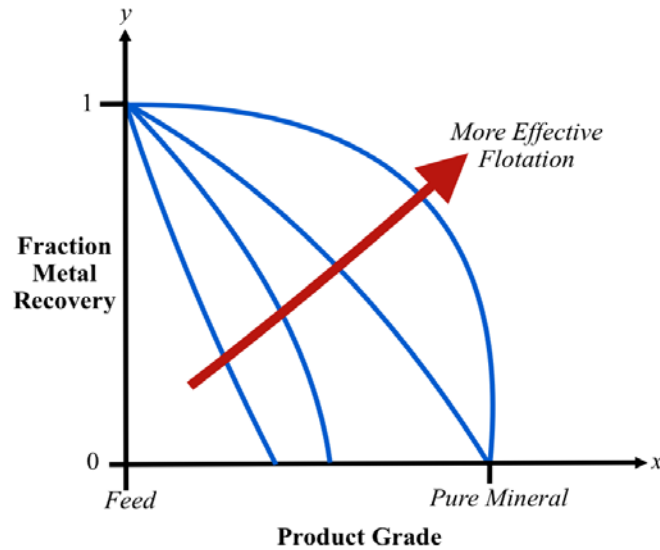


Figure 2.5 Typical grade-recovery curve

3 Microwave Treatment of Minerals

3.1 Thermally Assisted Liberation (TAL)

Thermally assisted liberation is the process of cyclical heating and cooling rocks to promote intergranular fracture (as opposed to transgranular fracture) as shown in Figure 3.1, due to thermal stresses within the mineral lattice caused by the repeated expansion and contraction of the structure (Fitzgibbon and Veasey, 1990; Vorster, 2001). This in turn increases the liberation of valuable minerals (Fitzgibbon and Veasey, 1990). Many researchers reported that thermal pre-treatment can weaken the grain boundaries; consequently, there is a reduction of fines in downstream processing, an increase in ore grinding, an increase in liberation, and a reduction in plant wear (King and Schneider, 1998; Veasey and Wills, 1991; Vorster, 2001; Walkiewicz et al., 1988; Walkiewicz et al., 1993; Walkiewicz et al., 1989). However, it would still be inefficient in terms of energy (Veasey, 1986; Veasey and Wills, 1991).

In conventional TAL, the entire ore is heated. In contrast, when an ore is heated in the microwave, the ore's dielectric properties are used which causes specific mineral phases to respond at different rates (Vorster et al., 2001). This is explained in greater detail in Chapter 2.2. Güngör and Atalay wrote that "to create cracks and micro-fractures at the mineral grain, the ore must be composed of minerals which have different heating characteristics when they are exposed to microwave radiation" (Güngör and Atalay, 1998). Additional advantages of using microwave assisted TAL are volumetric heating instead of surface absorption (which is the case with conventional heating), uniform heating, and high heating rates (Bonometti, 1998).

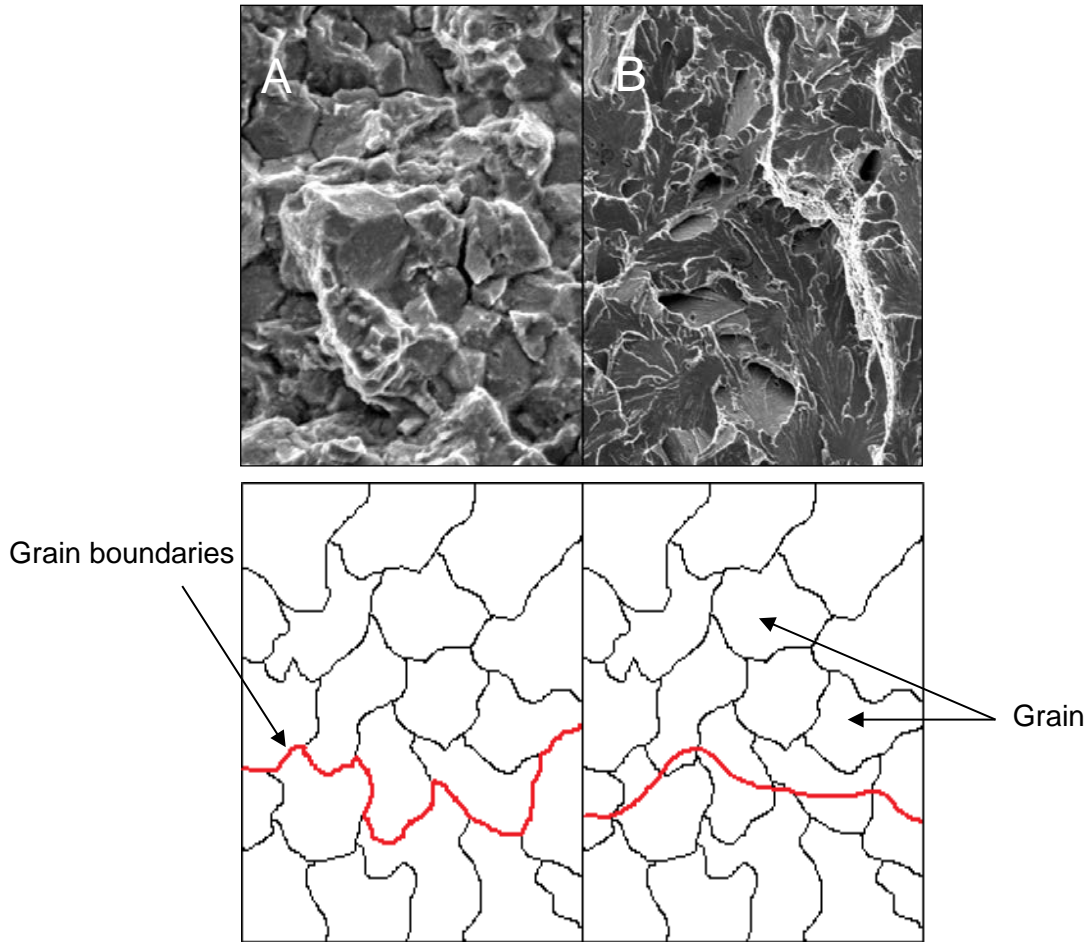


Figure 3.1 Schematic of two types of fractures a) intergranular fracture b) transgranular fracture

3.2 Microwaves

Microwave radiation is part of the non-ionizing electromagnetic spectrum with frequencies ranging from 300 MHz to 300 GHz (Haque, 1999). In 1946, Percy Spencer noticed the heating effects of microwaves while working with a vacuum tube called a magnetron. The microwave is composed of four basic components: a power supply, a magnetron, an applicator or oven, and a waveguide to transport the microwave from the generator to the applicator as shown in Figure 3.2 (Smith et al., 1984). Materials can be divided into three categories with respect to their

behaviour when exposed to microwave radiation: conductors, insulators and absorbers as shown in Table 1 (Church et al., 1988).

There are two main mechanisms responsible for the increase in temperature: ionic conduction and dipolar species rotation; there is a third mechanism called interfacial polarization which is a combination of the first two mechanisms (Kingston and Jassie, 1989). In ionic conduction the dissolved ions, oscillate when subjected to an electromagnetic field creating an electric current that faces resistances due to collisions with ions with neighbouring molecules or atoms; this causes an increase in temperature of the material (Metaxas, 1996). In dipolar rotation, the dipoles realign themselves by rotating with the electromagnetic field (Anwar et al., 2015). To achieve the thermal effect, the phase difference between the rotating dipoles and the electromagnetic field orientation causes molecular friction and collisions which causes the dielectric heating (Kappe et al., 2012). The heating depends on the ratio of the “loss factor” to the dielectric constant of the material. The dielectric constant is the measure of the ability of the material to delay the microwave energy as it passes through it (Haque, 1999). The “loss factor” is a measure

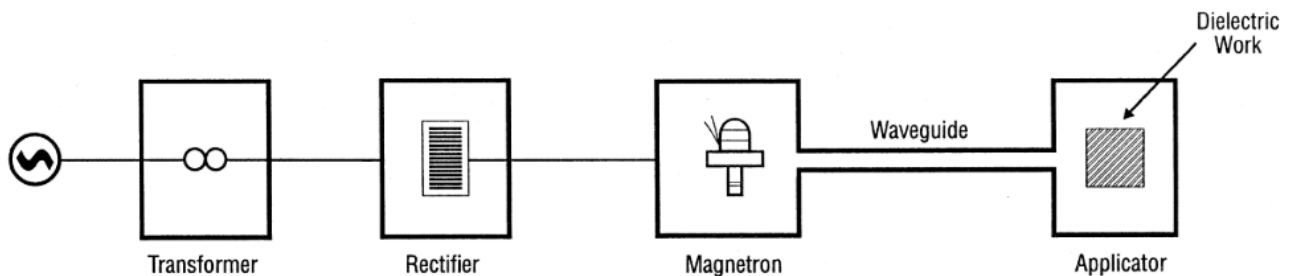
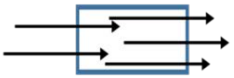
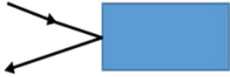
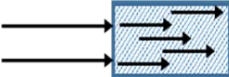


Figure 3.2 Simplified Microwave Heating System

of the loss of energy in a dielectric material through dissipative phenomena (Collin, 1966).

Table 3-1 Interaction of Microwave Radiation with Different Materials

	Material Type	Penetration
	Transparent (No heat)	Total transmission
	Reflective (No heat)	None
	Absorber (Materials are heated)	Partial to total absorption

3.2.1 Factors Affecting Dielectric Heating

Microwave heating depends on various factors including dielectric permittivity, conductive losses, temperature, sample geometry, field intensity, and the cavity design. There may also be interactions between the factors (Vorster, 2001).

3.2.1.1 Dielectric Properties

Permittivity of a material is a complex number with a real component (ϵ' , dielectric constant) and an imaginary component (ϵ'' , termed dielectric loss factor). These two components are used to express the dielectric response of materials in electromagnetic fields. The dielectric constant is the ability a material has to store microwave energy. The loss factor is the ability a material has to dissipate the stored energy (Al-Harahsheh et al., 2009; Anwar et al., 2015; Metaxas et al., 1988). Permittivity (ϵ^*) is given by the following equation:

$$\epsilon^* = \epsilon' - j\epsilon'' \quad (6)$$

Where $j = \sqrt{-1}$. Alternatively,

$$\epsilon^* = \epsilon_0(\epsilon'_r - j\epsilon''_{\text{eff}}) \quad (7)$$

Where ϵ_0 is the permittivity of free space ($8.86 \times 10^{-12} \text{F/m}$), ϵ'_r is the relative dielectric constant, ϵ''_{eff} is the effective relative dielectric loss factor.

The amplitude of an electromagnetic wave decreases as it propagates into a dielectric material because the power is absorbed by the material. The field intensity and the associated power flux density decreases exponentially with distance from the surface when there is an absence of reflection. The rate of decay of the power dissipation is a function of relative permittivity and the loss factor. The penetration depth (D_p , m) is defined as the distance from the material surface where the absorbed electric field falls to $1/e$ of the electric field at the surface. D_p is given by (Church et al., 1988; Schiffmann, 1995):

$$D_p = \frac{c}{2\pi f \sqrt{2\epsilon'} \left[\sqrt{1 + \left(\frac{\epsilon''_{\text{eff}}}{\epsilon'_r} \right)^2} - 1 \right]^{1/2}} \quad (8)$$

The average power density P_d (volumetric absorption of electromagnetic energy W/m^3) produced in a non-magnetic material when exposed to electromagnetic energy is defined as (Al-Harashseh et al., 2009):

$$P_d = 2\pi f \epsilon_0 \epsilon''_{\text{eff}} E^2 \quad (9)$$

where E is electric field strength inside the material (V/m).

3.2.1.2 Temperature and Frequency

The temperature of a material increases as the material absorbs microwave energy. The rate at which the temperature changes is given by:

$$\frac{dT}{dt} = \frac{P}{C\rho} \quad (10)$$

Where C is the specific heat in $\text{J/K}\cdot\text{kg}$ and ρ is the density in kg/m^3 .

Materials can exhibit physical and chemical changes that alter the interaction of microwaves with the material which is why the variation of material dielectric properties with temperature is important (Meredith, 1998). In general, the variation of ϵ' and ϵ'' in material subjected to the microwave heating is related to the heating mechanism in the material (Atwater and Wheeler, 2004). A temperature increase will increase both ϵ' and ϵ'' because the dipoles can flip faster because of a decrease in dielectric relaxation (Böttcher et al., 1974; Hall et al., 1998; Kobusheshe, 2010). Dielectric relaxation is the time it takes for dipoles to return to random orientation when the electric field is removed (Sebastian and Jantunen, 2008). For most materials, it is difficult to predict the variation of the dielectric properties with temperature. This is because as temperature changes the heating mechanism may also change. Consequently, the dielectric properties of materials are usually measured over a temperature range. Figure 3.3 and Figure 3.4 show the results of the variation of ϵ' and ϵ'' with temperature for minerals measured at 2.216 GHz (Cumbane, 2003; Kingman et al., 2004). It can be seen that galena and sphalerite show little variation with temperature; whereas, pyrite, chalcopyrite, and chalcocite show significant variation in the specific temperature range related to phase transformation, in the form

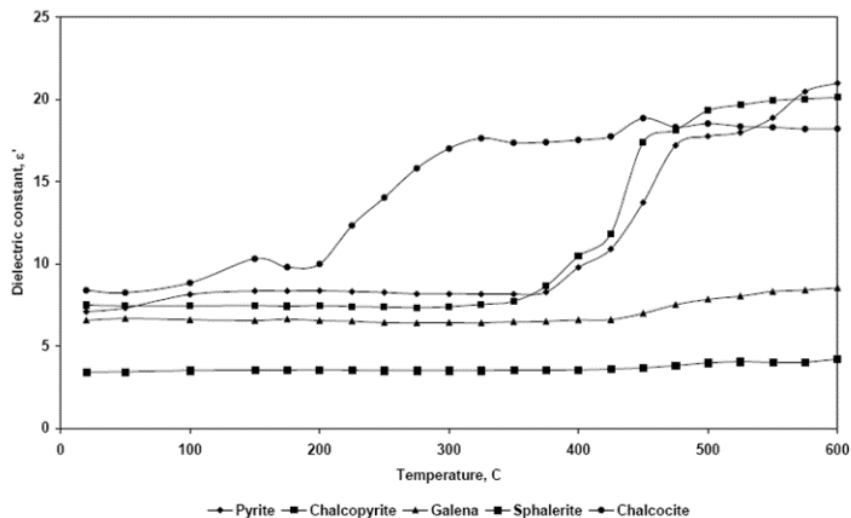


Figure 3.3 Variation of dielectric constant with temperature for selected minerals (Kobusheshe, 2010)

of oxidation.

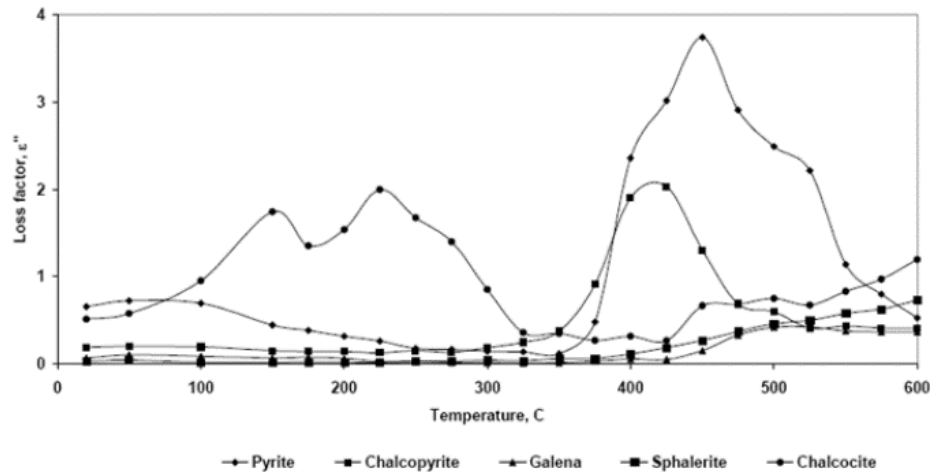


Figure 3.4 Variation of loss factor with temperature for selected minerals (Kobusheshe, 2010)

3.2.1.3 Particle Size

As noted in the previous section, different materials respond differently to dielectric heating. Several studies have demonstrated the effect of particle size on heating properties (Chanaa et al., 1994; Kingman and Rowson, 1998; Walkiewicz et al., 1988). It has also been reported that particle size was an important, but not necessarily consistent, factor in the heating of granular material. Walkiewicz and Chanaa found that finer particles respond better to microwave radiation than the larger particles. However, it was also observed that fine Al_2O_3 heated faster than coarse Al_2O_3 , but coarse Fe_3O_4 heated faster than fine Fe_3O_4 (Standish et al., 1991).

3.3 Use of Microwaves in Mineral Processing

The effect of microwave radiation on enhancing mineral liberation has been extensively studied in recent years. The effect of microwave radiation on forty minerals was investigated by Chen et al. which showed the different heating capacities of the different minerals; some minerals heat faster than others (Chen et al., 1984; Walkiewicz et al., 1988). Thus, by changing the properties

of minerals using microwave radiation could lead to better processing of ores. Microwave radiation could show benefits in comminution, magnetic separation, leaching, and froth flotation.

Fractures produced at the grain boundaries of two or more minerals expand at different rates because of the differential heating. Consequently, the energy required to crush the ore and liberate the mineral grains is reduced when an ore is exposed to microwave radiation prior to comminution stage. In addition, increasing the power levels decrease the Bond Work Index (BWI) which means that less energy will be required to grind the ore (Marland et al., 2000; Sahyoun et al., 2004).

Microwave heating can induce phase changes at the grain boundaries of minerals which can alter the magnetic properties of minerals (Koleini and Barani, 2012). Kingman et al. showed that some minerals such as chalcopyrite, hematite, and wolframite exhibit an increase in the magnetic susceptibility after being exposed to microwave radiation (Kingman et al., 2000). This increase in susceptibility has also been observed by Lovas et al. for tetrahedrite and by Znamenackova et al. for pyrite (Lovás et al., 2003; Znamenáčková et al., 2005), consequently leading to an increase in the effectiveness of magnetic separation.

Microwave assisted leaching of copper, gold, nickel, cobalt, manganese, lead, and zinc were examined by Al-Harashsheh and Kingman. It was found that microwave pre-treatment improved the extraction efficiency of metals by reducing leaching time and increased the recovery of valuable metals (Al-Harashsheh and Kingman, 2004). Krishnan et al. investigated the effect of microwave irradiation on the leaching of zinc from sphalerite/pyrrhotite concentrate from India. It was observed that the zinc leaching was rapid, iron dissolution increased, and there was significant selectivity of zinc over iron (Krishnan et al., 2007).

The surface chemistry of the mineral has a great impact on the efficacy of froth flotation. Consequently, any alteration of the mineral surface due to exposure to microwave radiation will significantly influence the flotation process (Vorster et al., 2001). For example, sulfide minerals can undergo oxidation and phase changes on the surface of the mineral when exposed to an oxygen rich environment. This change on the surface can decrease the flotation recovery (Sahyoun et al., 2003). In contrast, ilmenite recovery increased after exposure to microwave radiation because the oxidation at the surface increased the adsorption of the oleate ions onto the ilmenite surface (Fan and Rowson, 2000, 2002).

4 Physicochemical Properties of Minerals

The understanding of the physicochemical properties of minerals is essential for the efficient separation of valuable minerals from gangue during the concentration stage.

4.1 Surface Chemistry

Solid particles in an aqueous suspension will develop a surface charge and a surface potential due to factors such as surface group ionisation, preferential dissolution of ions, ion adsorption to the surface and isomorphous substitution in the mineral lattice (Jordens et al., 2014a; Riley, 2009). These two aspects are important in the separation processes of mineral slurries. At the same pH and salt concentration, all pure particles of the same material will have the same surface charge in the suspension (Waters et al., 2008). Consequently, if the charges are strong enough to overcome the attractive Van der Waals forces, they will naturally repel each other. However, if the Van der Waal forces are dominant, then aggregation will occur which will lead to the particles settling.

The DLVO theory (after Derjaguin, Landau, Verway, and Overbeek) looks at the balance between electrostatic repulsion forces (V_R) due to the electrical double layer and Van der Waals attractive force (V_A) to explain why some colloidal systems coagulate while others do not (Sharma, 2016; Trefalt and Borkovec, 2014) as shown below:

$$V_T = V_R + V_A \quad (11)$$

$$V_R = 2\pi\epsilon a \zeta^2 e^{-\kappa D} \quad (12)$$

Where D is the particle separation; a is the particle radius [m]; π is the solvent permeability; κ is a function of the ionic composition; ζ is the zeta potential [mV].

$$V_A = \frac{-A}{12\pi D^2} \quad (13)$$

Where A is the Hamaker constant.

Figure 4.1 shows the total DLVO profile comparing the Van der Waals and double layer contributions. Van der Waals forces dictate the profiles at large and small distances while the double layer forces dominate the intermediate distances. The combination of these forces with the DLVO profile results in a deep attractive well known as the primary minimum. At larger distances, the energy profile goes then through a maximum, and subsequently passes through a shallow minimum where there is a high salt concentration, which is referred to as the secondary minimum

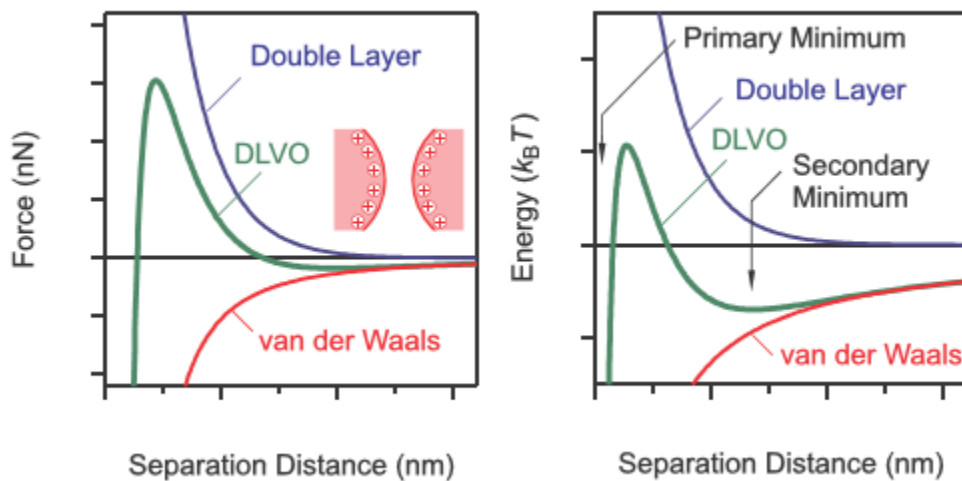


Figure 4.1 The change in free energy as a function of particle separation (Trefalt and Borkovec, 2014)

minimum (Riley, 2009; Sharma, 2016).

4.1.1 Zeta Potential

The surface charge of a particle in suspension can be difficult to measure directly, but it is possible to define a plane of shear where the counter ions are sufficiently attracted to the particle surface that they will move with the particle when the particle is set in motion (Jordens et al., 2014b). The electrochemical potential decreases as a function of distance from the particle surface, and the potential that is measured at the plane of shear is referred to as the zeta potential (ζ) (Fuerstenau and Pradip, 2005; Riley, 2009). This is shown in Figure 4.2.

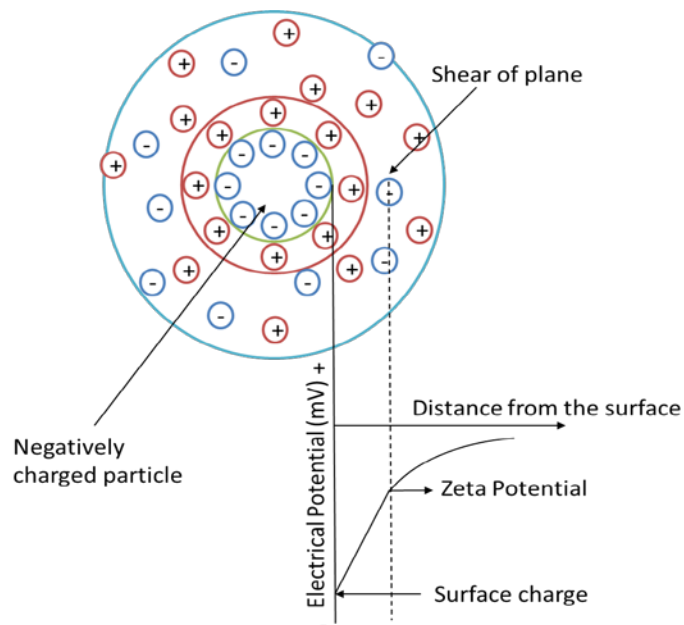


Figure 4.2 Diffuse double layer of a mineral particle with the point of measurement of zeta potential

The isoelectric point (IEP) is often used to characterize the electrical double layer as it allows the prediction of the sign of the charge on a surface in a given pH range (Pope and Sutton, 1973). The IEP is the pH at which the zeta potential is equal to zero. As the pH becomes more acidic, the zeta potential becomes more positive, and vice versa. This characteristic of the electrical double layer can provide important information about the mineral surface in flotation. Understanding the zeta potential of a mineral, the IEP, and the collector's ionization behaviours at various pH in an aqueous condition allows one to predict the mechanism of collector

adsorption on the mineral surface (Chunpeng, 1993; Marion et al., 2015). This relationship can be seen in Figure 4.3. The two most common methods of determining the zeta potential are through electroacoustic and electrophoretic techniques.

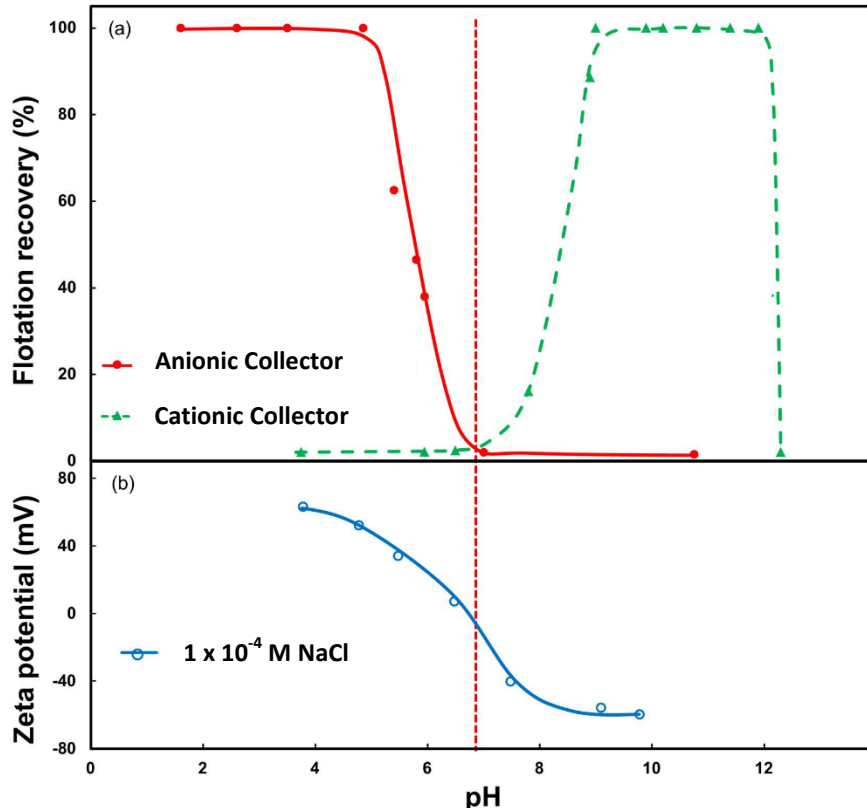


Figure 4.3 (a) Flotation response of a mineral to two different collectors - anionic and cationic - as a function of pH (b) surface charge as a function of pH. 1×10^{-4} M NaCl is the background electrolyte to keep a constant ionic strength. (Wills and Finch, 2016)

4.1.1.1 Electroacoustics

When a high frequency AC field is applied to a colloidal solution, both the particles and the diffuse layer are set in motion. As the inertia of particles differs to that of the diffuse layer the velocity/field transfer function differs for the two components. This results in pressure waves. Taking the measurements of the sound, the zeta potential can be determined. This method can be used with optically dense systems (Hunter, 1998; O'Brian, 1988; Riley, 2009).

4.1.1.2 Electrophoretics

Zeta potential measurements are obtained by determining the electrophoretic mobility, μ , of a particle in solution when an electric field is applied (Riley, 2009). This technique is known as electrophoresis. The electrophoretic mobility is correlated to either the Smoluchowski equation or the Hückel equation to obtain the zeta potential (Trefalt and Borkovec, 2014). Both the equations relate the zeta potential and electrophoretic mobility to the viscosity of the background electrolyte, η , and to the electric permittivity of the medium, ϵ . Hückel equation is used for a large double layer relative to the particle size (Waters, 2007). Hückel's equation is as shown below:

$$\mu = \frac{2\epsilon\zeta}{3\eta} \quad (14)$$

Smoluchowski equation is as shown below:

$$\mu = \frac{\epsilon\zeta}{\eta} \quad (15)$$

4.2 Magnetism

There are three main forms of magnetism for minerals: diamagnetism, paramagnetism, and ferromagnetism. Diamagnetic materials do not have any unpaired electrons. When a magnetic field is applied to the material, a magnetic moment can be induced. In the material, the direction of the magnetic moment is opposite that of the magnetic; consequently, the magnetic effect is cancelled out (Premaratne, 2004). Examples of diamagnetic materials are quartz and calcite. Paramagnetic materials have a magnetic dipole moment because the magnetic effect does not cancel out. The dipoles align with the applied field, creating magnetisation. However, the alignment is not perfect because there are thermal vibrations within the solid atoms caused by the change in temperature (Barani et al., 2011; Bluhm et al., 1986). Materials that are ferromagnetic

have one of two characteristics. First, the materials have perfect alignment of the magnetic dipoles with the applied field. There are five known ferromagnetic elements at room temperature: iron, cobalt, nickel, gadolinium, and dysprosium. In the elements, the adjacent atoms couple their magnetic moments in parallel causing an exchange coupling. This coupling disappears when the element is heated to a temperature above the Curie Temperature (T_c) and the material becomes paramagnetic (Andriese et al., 2011; Barani et al., 2011; Uslu et al., 2003). Second, the material has magnetic memory known as remanence which is the residual magnetisation after the applied field has been turned off. When a reverse magnetic field is applied, the magnetisation can be reduced to zero. This is known as the coercivity (Barani et al., 2011; Premaratne, 2004; Uslu et al., 2003; Waters, 2007; Waters et al., 2007; Waters et al., 2008).

4.2.1 Magnetic Moment

The magnetic moment of a sample can be obtained using a vibrating sample magnetometer (VSM). The magnetic moment is a vector quantity that lines up with the external magnetic field to determine the torque.

4.2.2 Magnetisation

The magnetic moment is measured and converted to magnetisation:

$$M = \frac{\mu}{V} \quad (16)$$

Where M is the magnetisation (A/m), μ is the magnetic moment (Am^2), and V is the volume of the sample (m^3). Paramagnetic samples will have a linear relationship whereas ferromagnetic samples will initially increase, then level off at the saturation magnetisation (M_s). Figure 4.4 illustrates a theoretical hysteresis loop. Increasing the field strength to above the saturation point

would produce a recovery that is relatively lower when considering the higher energy consumption.

The magnetic behaviour of a material is usually shown by a hysteresis loop which plots the variation of the magnetisation (M) with the applied magnetic field intensity (H) (Barani et al., 2011). As shown in Figure 4.4, the magnetisation of ferromagnetic samples reach a saturation point called the saturation magnetisation (M_s) where the magnetisation is constant with increasing field strength. If the magnetic field is reduced, the relationship will follow a different curve towards zero field strength at which point it will be offset from the original curve by an amount called the remanence magnetism (M_r) (Robert and Handley, 2000). When the magnetization is completely removed, coercivity is obtained (H_c). Paramagnetic materials have a

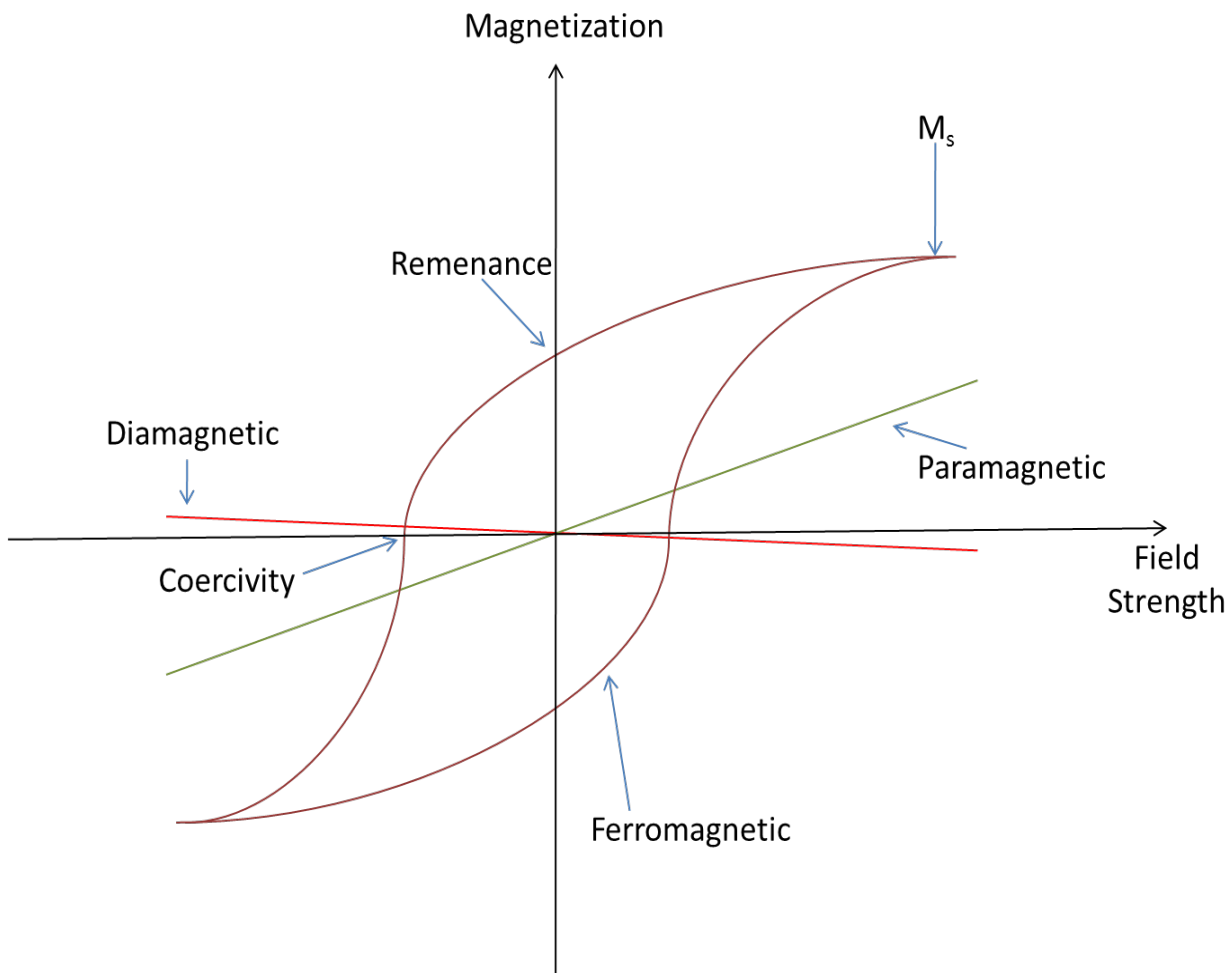


Figure 4.4 Magnetization of different magnetic materials

linear relationship between the magnetisation and the field strength (Znamenáčková et al., 2005).

4.2.3 Magnetic Susceptibility

susceptibility is a dimensionless parameter that indicates whether a material is attracted to or repelled by the applied magnetic field. It is the ratio of magnetisation (M) to the applied magnetic field intensity (H) (Wills and Finch, 2016):

$$\chi = \frac{M}{H} \quad (17)$$

Diamagnetic materials have a constant negative magnetic susceptibility; whereas paramagnetic materials have a positive magnetic susceptibility. The magnetic susceptibility of ferromagnetic

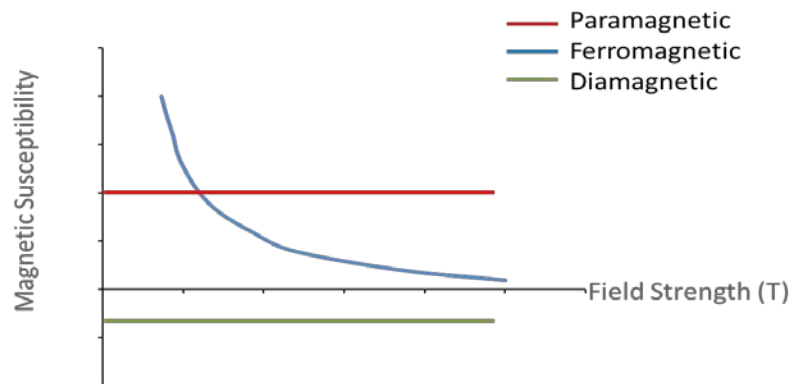


Figure 4.5 Magnetic susceptibility versus field strength for a diamagnetic, paramagnetic, and ferromagnetic material

materials depend on the magnetic field. This is shown in Figure 4.5.

4.2.4 Vibrating Sample Magnetometer (VSM)

The magnetic moment of a sample can be determined by a vibrating sample magnetometer (VSM) which was invented by Simon Foner (Foner, 1956). The main components of the VSM are the vibrating rod and the detection coil. The detection coil is attached to the poles of the

electromagnet. As the sample vibrates, the field lines generated by the sample cut through the detection coil. The magnetic moment is then measured. A schematic of the VSM is illustrated in **Error! Reference source not found..**

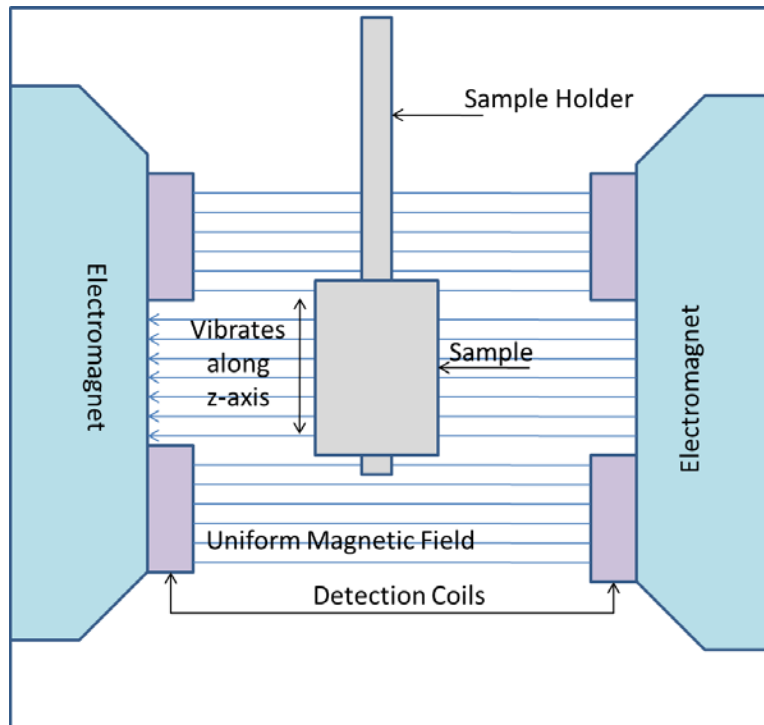


Figure 4.6 Schematic of a vibrating sample magnetometer

5 Methodology

5.1 Introduction

This chapter is about the methodologies that were used throughout the experimental processes.

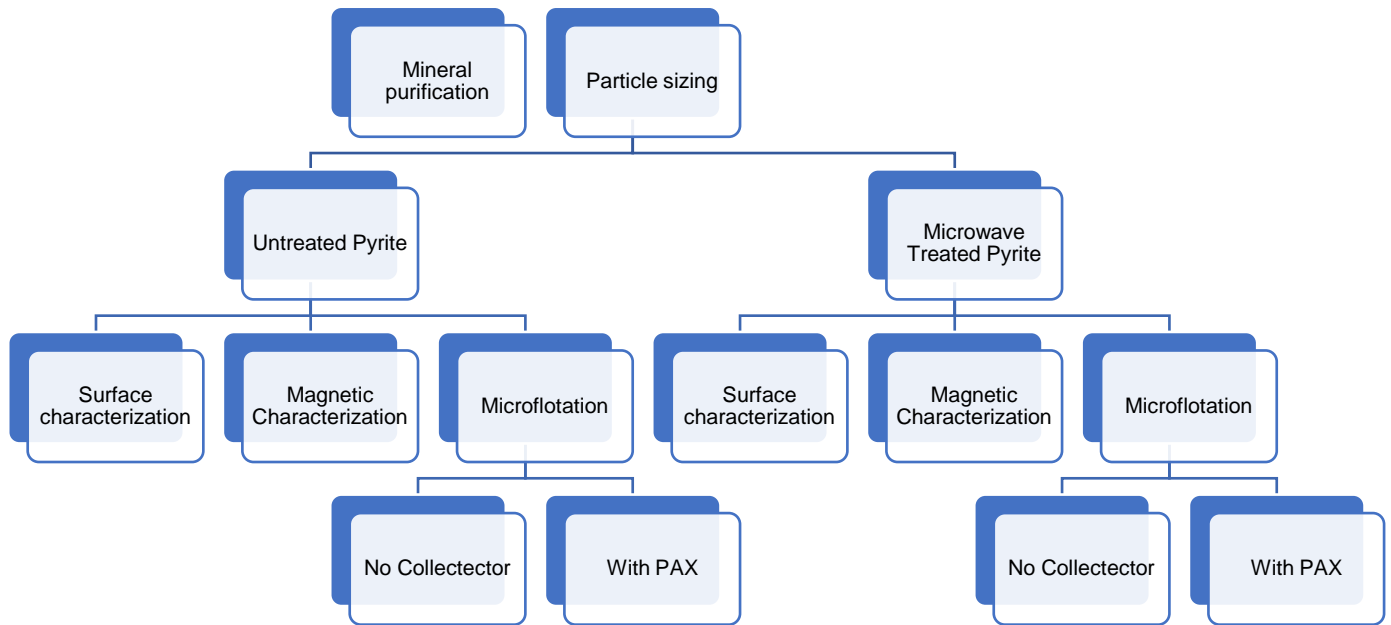


Figure 5.1 Experimental Steps

Figure 5.1 illustrates the experimental steps.

5.2 Materials

5.2.1 Pyrite

Pyrite is a weakly paramagnetic mineral that has a cubic crystal structure where cation and anion sites are replaced with Fe^{2+} ions and S_2^{2-} . Each S atom is coordinated to three Fe atoms and one

S atom. Fe is octahedrally surrounded by six S atoms. It has 2 types of bonds that are predominantly covalent: the Fe-S and the S-S bonds (Nesbitt et al., 1998).

It has been reported that sulfides follow the order below for spontaneous oxidation (Sutherland and Wark, 1955):



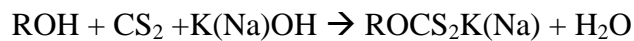
It is clear that pyrite tends to oxidize readily in air. It has been reported that pyrite is in an electrochemically passive state when exposed to air (Majima, 1971). A film forms at the surface which may be absorbed oxygen or oxygen-sulfur compound (Dimou, 1986; Majima, 1971). In an aqueous solution, the products of oxidation in acidic pH range are Fe^{2+} , H^+ , and SO_4^{4-} . Elemental sulfur can also be present in the pyrite system at very low pH ranges (Majima, 1971). Suzuki reported that a single grain of pyrite can have a mosaic of anodic and cathodic areas (Suzuki, 1967).

The preparation procedures prior to the separation stage also have a significant effect on the surface of pyrite. Haradat noted that the type of grinding had serious effects on the flotation recovery of pyrite (Dimou, 1986).

Pure pyrite sample was purchased from Wards Scientific (USA). The sample was kept in a freezer to decelerate the oxidation process due to contact with air.

5.2.2 Potassium Amyl Xanthate (Collector)

Xanthates are a product of alcohols, carbons disulfide and sodium or potassium hydroxide as shown in the reaction below (Bulatovic, 2010):



The stability of xanthate in an aqueous solution depends on the solution pH, the carbon chain length, and the concentration of xanthate (Fuerstenau, 1982). Xanthates decomposing rate decreases with increasing pH with the slowest being from pH 8 to 12. It is a first order reaction with respect to the concentration of xanthate (Granville et al., 1972). In the acidic region, xanthate hydrolyses and forms ethyl xanthic acid (HEX) and alcohol (ROH) (Dimou, 1986). In the alkaline region, xanthate ions decompose very slowly; consequently, they are more stable during flotation (Harris, 1984). Oxygen and heavy metal ions such as Fe^{3+} and Cu^{2+} can oxidize xanthate ions and produce dimer dixanthogen (Fuerstenau, 1982).

Xanthate acts as a sulfide collector by rendering the surface hydrophobic; consequently, floating the mineral. It has been determined through radiometric techniques that dixanthogen species absorb on the surface of pyrite (Fuerstenau et al., 1968; Gaudin et al., 1956).

The role of adsorption of xanthates of differing carbon chain length on pyrite was studied, and it was observed that the adsorption increased with the carbon chain length (Fuerstenau, 1982). It was also observed that up to pH 8 there is adsorption of the short chain xanthates. Moreover, it was found that the longer chain xanthates have a stronger interaction with the surface of pyrite (Dimou, 1986). Thus, potassium amyl xanthate (PAX) was chosen as the collector.

The concentration used also affects the adsorption onto the surface of pyrite (Ball and Rickard, 1976). A ten fold increase in the hydroxyl ion concentration was observed for a constant adsorption density which required a similar increase in collector concentration (Gaudin et al., 1956). Thus, a stronger interaction between pyrite and xanthate can be observed with an increase in xanthate concentration.

PAX was obtained from Prospect Chemicals (Canada), and used as a collector. PAX solution were prepared by dissolving the solids in deionized water. Potassium hydroxide and nitric acid were purchased from Fisher Scientific (USA) for use as pH modifiers (0.1 M to 1.0 M).

5.3 Sample Preparation

Pyrite obtained for this work was analysed using XRD to determine the mineralogical composition. The sample was found to be 73% pure with the major gangue mineral identified as calcite.

5.3.1 Mineral Purification

Based on the magnetic properties of the gangue minerals found in the pyrite sample, a Frantz Isodynamic Separator (Frantz, USA) was used to separate the various mineral phases based on their magnetic properties. The sample was stage pulverized then wet screened to remove particles less than 25 μm . The resultant size range of 38 μm to 425 μm was obtained. The various size fractions were passed through the Frantz Isodynamic Separator at a forward slope of 27.6° and a side slope of 15.1° to remove the unwanted ferromagnetic and diamagnetic minerals. The sample was processed at 0.12A.

The density of pyrite is 5.05 g/cm^3 and the density of calcite is 2.71 g/cm^3 ; therefore, a ratio of 1.85:1 for calcite:pyrite. Consequently, a laboratory Mozley Mineral Separator was used to separate the minerals with a low water flow rate. The light mineral was discarded. The heavy mineral was filtered, air dried on a pan. The product was then separated again by elutriation where water was used as the counter flow liquid. The calcite particles and pyrite fines went to the overflow and were discarded. The resulting sample was then sieved and separated in four particle size ranges: 212-425 μm , 75-212 μm , 38-75 μm , and 38-425 μm .

The purified pyrite was analysed using XRD. Rietveld analysis was conducted on the samples which showed >88% pure pyrite which was used for the remainder of the experimentations.

5.4 Microwave Treatment

The pyrite sample was crushed and ground to four particle size ranges: 38 to 75 μm , 75 to 212 μm , 212 to 425 μm , and 38 to 425 μm . In an alumina crucible, 20 g of pyrite sample was treated in a microwave oven at three different power levels – 0.8 kW (Panasonic High Power), 1.25 kW (Danby Design), and 3 kW (Amana Commercial RC30S) – at exposure times of 0s, 5s, 10s, 15s, and 30s. The sample was placed in the middle of the microwave oven. Once the treatment was completed, the hot crucible was removed using tongs. The bulk temperature of the microwave treated sample was measured by inserting a thermocouple into the hot material immediately after turning off the microwave power.

5.5 Surface Characterization techniques

5.5.1 X-Ray Diffraction (XRD)

X-ray powder diffraction is a rapid analytical technique primarily used for phase identification of a crystalline material. The analysed material was finely ground, homogenized, and the average bulk composition was determined. Bruker D8 Discovery X-Ray Diffractometer (USA) equipped with a copper tube as the x-ray generating source was used. Xpert High Score software was used to identify the peaks and the mineral phases present in the pyrite.

5.5.2 X-Ray Photon Spectrometer (XPS)

X-ray photoelectron spectroscopy is a surface chemical analysis technique that can be used to analyze the surface chemistry of pyrite. It is a surface-sensitive spectroscopic technique. XPS measurements were performed using K-Alpha surface analysis system (Thermo Scientific) with

an AlK α X-ray source (1489.6 eV), applying a 400 μ m diameter beam spot. To avoid charging on the surface, a flood gun was used to shoot the samples with low energy electrons during the experiments. The collected data was processed using Avantage Data Processing software (Thermo Fisher Scientific). The binding energy was calibrated using the background hydrocarbon C 1s binding energy of 284.8 eV; no binding energy correction was necessary for this study. The samples were dried in a vacuum oven before being transferred into the XPS analysis chamber.

5.5.3 Scanning Electron Microscope (SEM)

The surface topography and composition of the pyrite sample after microwave treatment were analysed with SEM Hitachi SU-3500 (Hitachi High-Technologies Corporation, Canada) equipped with EDS for micro detection of elements and crystal orientation. The surface maps were acquired at an accelerating voltage of 15 kV.

5.5.4 Vibrating Sample Magnetometer (VSM)

The vibrating sample magnetometer (VSM) measurements in this work were conducted using a LakeShore 7300 series VSM. All mineral samples were analysed intact. To conduct the measurements 50-100 mg of powdered sample was placed into the cylindrical VSM sample holder and attached to the end of an oscillating rod. The sample sits in the middle of four pick-up coils and a hall probe. The rod oscillates about this point as a magnetic field is applied to the sample to create a full hysteresis loop between +2 T and -2 T. Measurements are taken every 0.1 T. The magnetic moment as a function of magnetic induction is measured. Measurements of the empty sample holder were also conducted to ensure that any magnetic contribution of the sample holder may be subtracted from the sample data. The measured magnetic moment data as a function of magnetic field was converted into magnetisation. This was done by dividing by the

sample volume determined using theoretical density of pyrite (5020 mg/cc). The magnetic induction values are converted into magnetic field strength by dividing by the constant of permeability of free space, $4\pi \times 10^{-7}$ V s / A m.

5.5.5 Zeta Potential

Electrophoretic light scattering (ELS) zeta potential measurements were obtained using a NanoBrook 90Plus Zeta Particle Size Analyzer (Brookhaven Instruments, USA). There are many different types of contaminants that can ruin sample preparation such as dust. Improper sample preparation can lead to poor results due to the sensitivity of the instrument. Pyrite was ground to a particle size of smaller than $38\mu\text{m}$ and treated in a 3kW microwave oven for 0 seconds, 15 seconds and 30 seconds. Deionized water was used to clean all the beakers, electrodes, bottles, cuvettes, and syringe. A 20 mL bottle was filled with the electrolyte solution 10^{-2} M KNO_3 . A small amount of fine pyrite was added to the 20 mL electrolyte solution. The bottle was gently rocked to ensure that the pyrite was suspended in the solution. Finally, the sample cuvette was prepared for analysis. The cuvette was filled with the suspended pyrite solution and capped. The cuvette was then rocked back and forth to dislodge any dust attached to the interior of the cuvette and cap. The cuvette was then emptied to waste. This was done to avoid a dust laden surface. In the now empty cuvette, the pyrite solution was poured once more. Place the cuvette into the instrument and wait till sample equilibrium since variations in temperature can yield poor results. Zeta potential measurements were carried out from pH 3 to 11. At each new pH level, the suspension was allowed to equilibrate for 5 min. The suspension was also conditioned for 5 min. after the addition of the collector. In addition, new suspensions were made for titrations from natural pH to the acidic and basic regions. Five replicates were done for each pH. The background electrolyte used was 10^{-2} M KNO_3 .

5.6 Microflotation

Flotation was conducted through microflotation experiments using a modified Hallimond tube (34.6 cm in height, 3.3 cm outer diameter and 2.6 cm inner diameter) as shown in Figure 5.2.

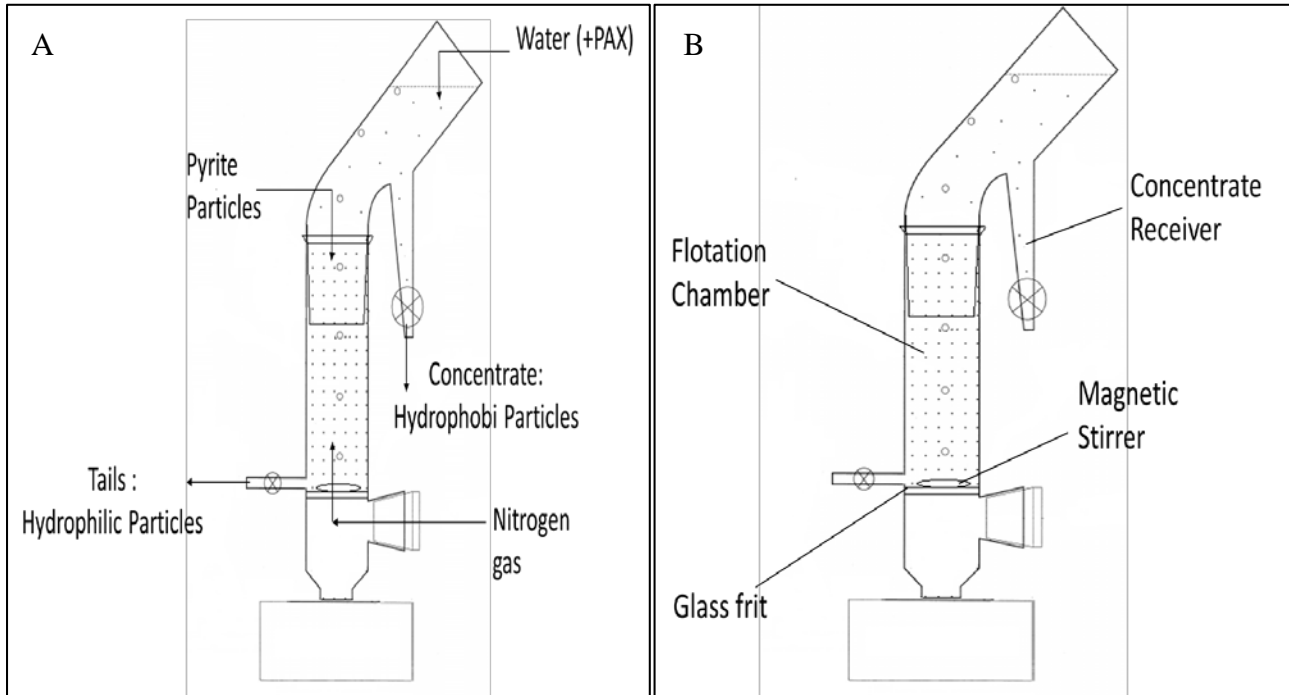


Figure 5.2 Schematic of the Modified Hallimond Tube (a) the process (b) parts

5.6.1 Single Mineral

The samples (1 g for each test) were conditioned with reverse osmosis water for 5 min. The suspension was then transferred to the microflotation cell and the volume was adjusted to 170 mL. During the microflotation tests, constant stirring was maintained by use of a magnetic stirrer to keep the particles in suspension. High purity nitrogen was used as the flotation gas at a flow rate of 40 mL/min to prevent any further oxidation while flotation tests were being conducted, and the recovered material was collected for one min after the first bubbles arrived at the surface of the suspension. The concentrate was collected from the top and the tailings were collected from the bottom. The microflotation experiments were run five times for each condition.

5.6.1.1 Single Mineral with collector

PAX was dissolved in deionized water and diluted to the desired concentration, ranging from 0- 10^{-4} M. The mineral samples (1 g for each test) were conditioned with 30 mL of PAX for 5 min. The suspension was then transferred to the microflotation cell and the volume was adjusted to 170 mL. During the microflotation tests, constant stirring was maintained by use of a magnetic stirrer to keep the particles in suspension. High purity nitrogen was used as the flotation gas at a flow rate of 40 mL/min to prevent any further oxidation while flotation tests were being conducted, and the recovered material was collected for one min after the first bubbles arrived at the surface of the suspension. The concentrate was collected from the top and the tail was collected from the bottom. The microflotation experiments were run five times for each condition.

6 Results

6.1 Temperature Analysis

Microwave heating characteristics of different size fractions of pyrite sample were determined at power levels of 0.8 kW, 1.25 kW, and 3.0 kW. The results are shown in Figure 6.1-Figure 6.3 as the bulk temperature of the sample after microwave irradiation duration of 5, 10, 15, 30, and 60 seconds.

As the figures show, the maximum temperature attained increased with increasing power and exposure time; however, the particle size did not affect the bulk temperature of the sample. The maximum bulk temperature of 531°C was observed at 3 kW with an exposure time of 60s. However, at this parameter, arcing was observed and some particles had fused together. Uslu and Atalay observed that the heating rate and the maximum attained temperature of pyrite samples increased with increasing power levels in decreasing particle size (Uslu and Atalay, 2003, 2004). They also observed that the maximum attained temperature and heating rate were lower in heatings under nitrogen instead of air because it hindered the contact of pyrite with oxygen in the air (Kelly and Rowson, 1995; Uslu et al., 2003). Wu observed that 10-20% presence of larger particles in the magnetic powder does not affect the overall microwave performance significantly; however, a large percentage causes a drastic decrease in permeability (Wu et al., 2005). Standish reported that particle size is an important but not consistent factor in the heating of granular material, for instance, fine Al₂O₃ heated faster than coarse Al₂O₃ but coarse Fe₃O₄ heated faster than fine Fe₃O₄ (Standish and Worner, 1990; Standish et al., 1990; Standish et al., 1991). Since there is little dependence on the particle size, the particle size range of -425+38 μm was used going forward.

Microwave absorption leads to an increase in temperature as observed in Figure 6.1 due to frictional heating caused by dipolar species rotation or by migration of ionic species. The heating of materials depends greatly on the ratio of the loss factor of materials to the dielectric constant. Materials with a high loss factor being easily heated by microwave energy. Pyrite can be heated relatively rapidly due to its associated high dielectric constant (Chatterjee and Misra, 1991; Marland et al., 2001)

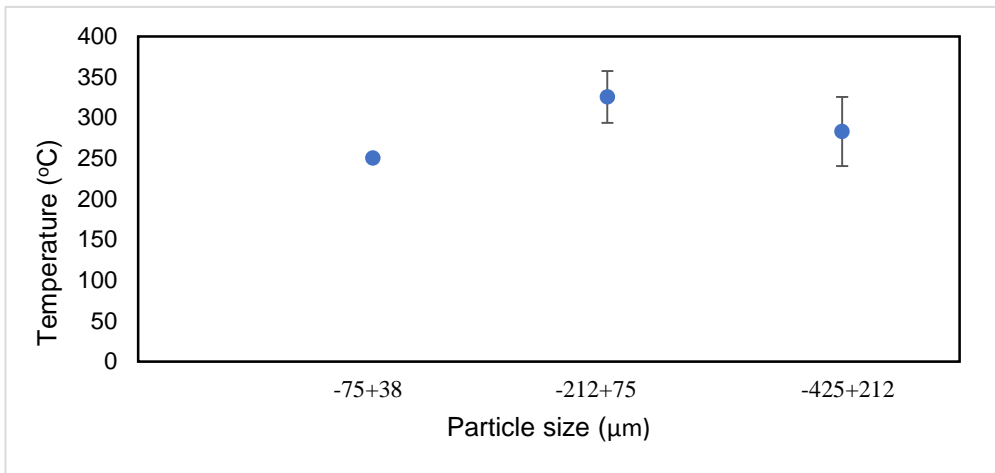


Figure 6.1 The effect of particle size on the bulk temperature of pyrite sample treated in a 3kW microwave oven for 10s.

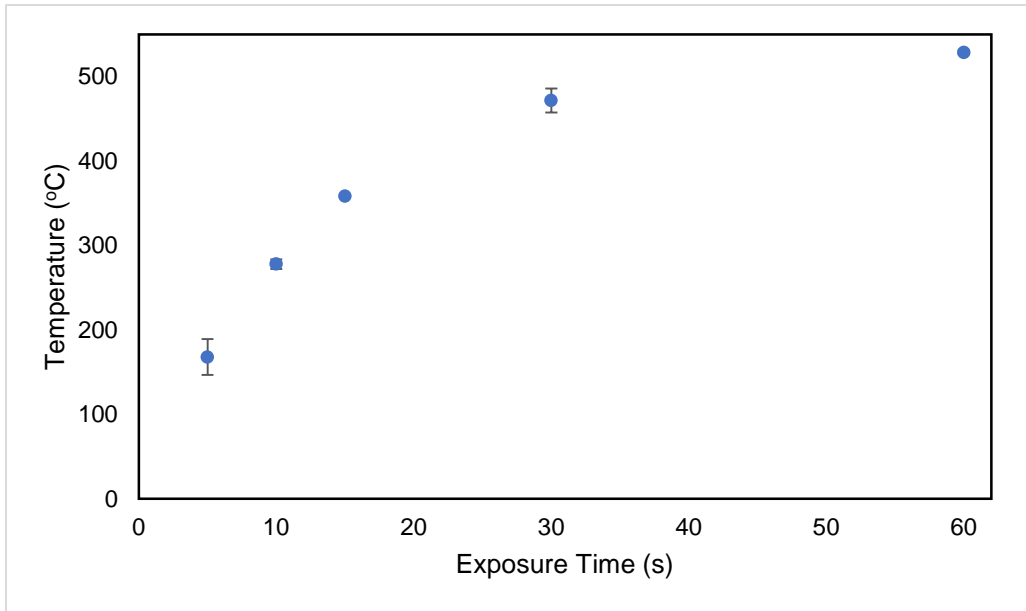


Figure 6.3 The effect of exposure time on the bulk temperature of -425+38 micrometer pyrite

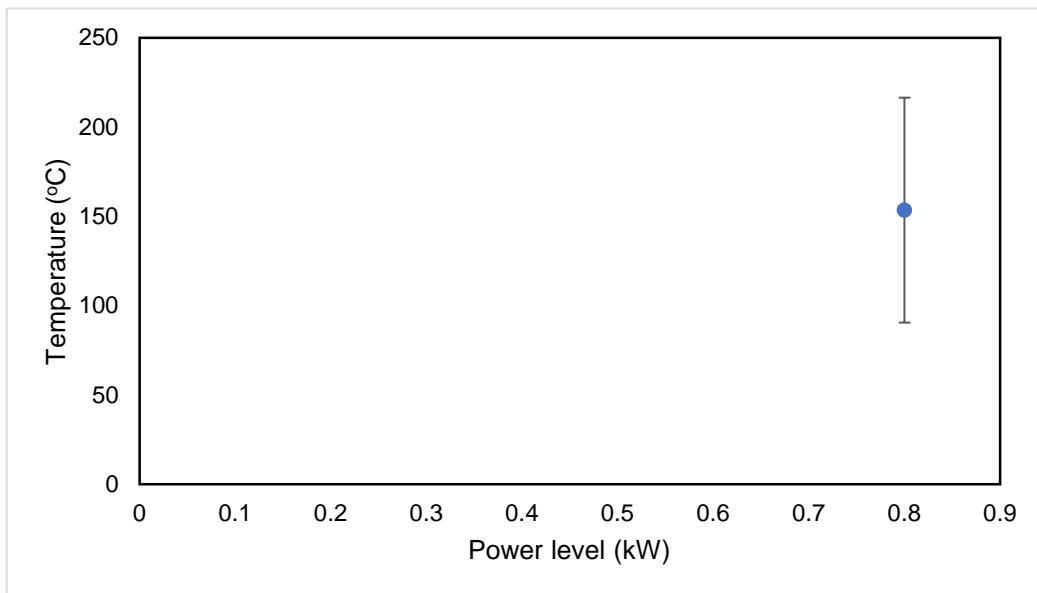


Figure 6.2 The effect of power level on the bulk temperature of -425+38 micrometer pyrite sample treated for 15s.

6.2 Surface Characterization

6.2.1 XRD

XRD analysis of the untreated pyrite showed some calcite peaks present. A Rietveld analysis showed that the samples was >88% pure pyrite After exposure to microwave radiation, the XRD

showed slight changes but nothing to definitively state the nature of the new phases being present. Figure 6.4 shows the XRD for untreated pyrite and the pyrite exposed to 3 kW microwave radiation for 5, 10, and 15s in the range of 20 to 120° for 2 θ . It can be seen in Figure 6.4 that while the height of the peaks changes with treatment. This is because the intensity of the diffraction peaks is determined by the arrangement of atoms in the entire crystal which could indicate some form of phase transformation. The position of the peaks remains the same and the position of any new peaks cannot be accurately identified. This can be because the changes are below the threshold of the XRD sensitivity which is approximately 5% of the sample volume. The lack of observable phase changes in XRD after microwave treatment was also observed by other authors (Sahyoun et al., 2003).

To understand the phase transformations and oxidation on the surface of pyrite after exposure to microwave radiation, other methods were employed such as X-ray photoelectron spectroscopy and scanning electron microscopy (Fandrich et al., 2007; Irannajad et al., 2014; Watts et al., 2003).

6.2.2 XPS

To determine if new phases were generated, the broadband spectrum of pyrite was examined to identify the elements that are present.

The binding energies that are identifiers of pyrite in the sulfur spectra are located at 162 eV as can be seen in Figure 6.5 (Naveau et al., 2006). This is also characteristic of elemental sulfur and oxidized sulfur (Laajalehto et al., 1999). The peak at approximately 168 eV indicates the presence of sulfoxy species such as sulfate and thiosulfate (He et al., 2005). The surface oxidation does not change much the proportion of sulfide in similar environments (Fairthorne et al., 1997).

In the iron spectra in Figure 6.4, the dominant peak is at 707 eV which is recognised as pyritic iron (Weisener and Gerson, 2000b). There is an emerging peak between 708 eV and 715 eV which can be attributed to ferric oxide or hydroxide (Weisener and Gerson, 2000a).

The binding energies of O 1s, S 2p, and Fe 2p components of XPS of the sample surfaces before and after different exposure times in a 3 kW microwave is shown in Figure 6.6. The oxygen components resulting from the oxidation of the mineral surface is observed in all the treated samples. A peak at 532 eV emerges for the treated sample. This peak is primarily due to sulfate, hydroxide, and sulfoxy species that are a result of oxidation on the surface of the mineral (Boulton et al., 2003; Deng et al., 2013). The peak at 530 eV is characteristic of FeOOH or oxide type oxygen (Fairthorne et al., 1997; Szargan et al., 1992).

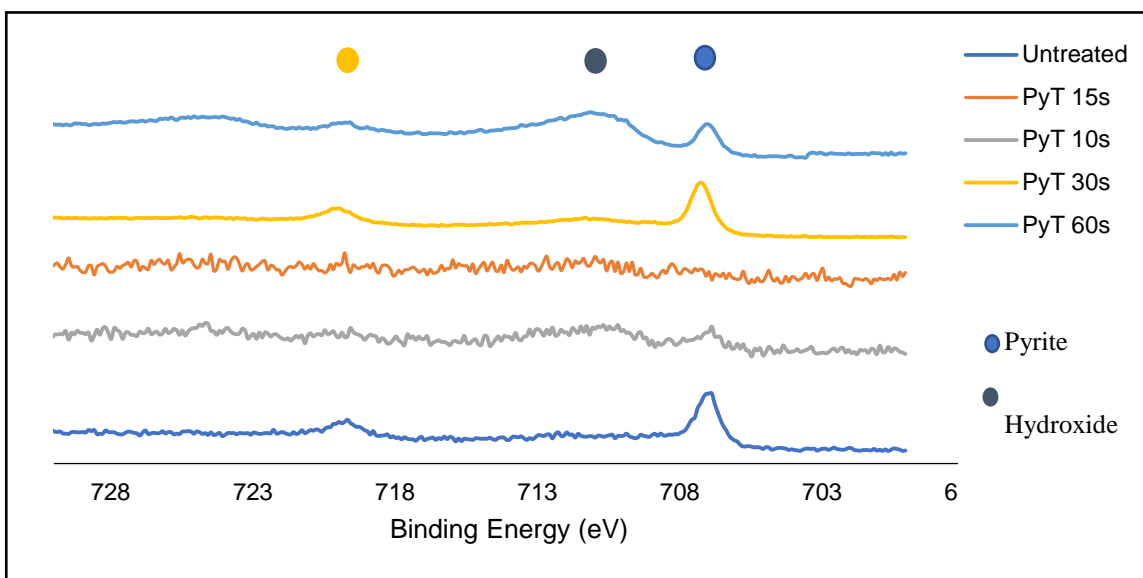


Figure 6.4 Iron spectrum of microwave treated pyrite and untreated pyrite from XPS showing the iron phases present

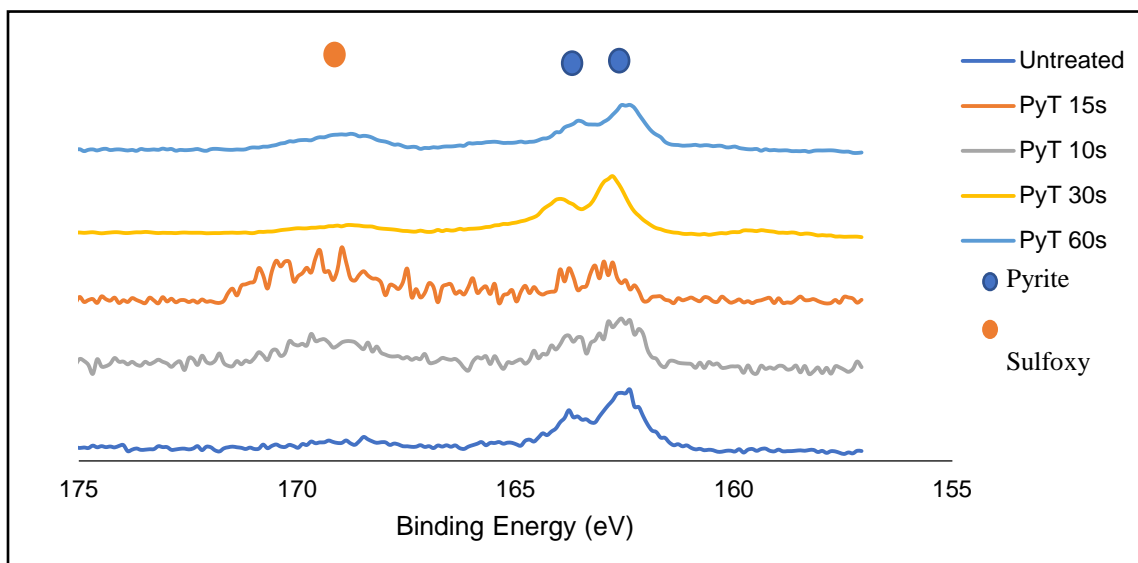


Figure 6.5 Sulfur spectrum of microwave treated pyrite and untreated pyrite from XPS showing the different sulfur phases present

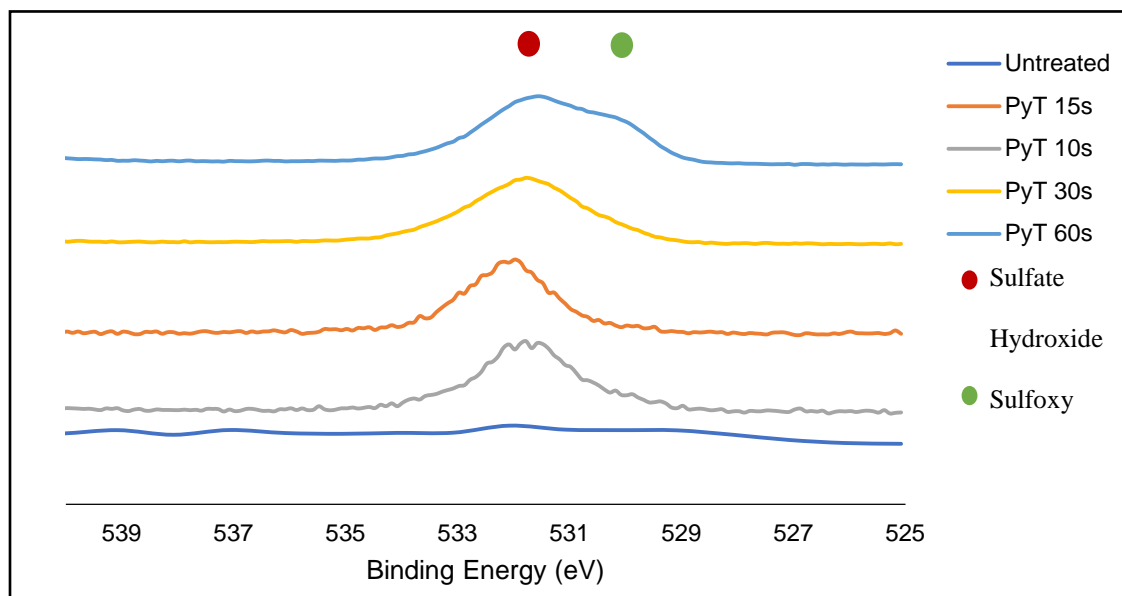


Figure 6.6 Oxygen spectrum of microwave treated pyrite and untreated pyrite from XPS showing the oxygen phases present

6.2.3 SEM

To better understand the new phases that formed, SEM images of the treated pyrite surface were as shown in Figure 6.9. It can be seen in left image of Figure 6.7 that after treatment for 30s in a 3 kW microwave, some pyrite particles have turned darker on the surface. This could indicate a phase change. In the right image of Figure 6.7 the cross section of the treated sample was seen through an optical microscope. It can be seen that the boundaries of the particles are darker because the only surface of the particle was primarily transformed. This is in agreement with Vorster who observed that oxidation occurred along the grain boundaries as can be seen in Figure 6.8 (Vorster, 2001).

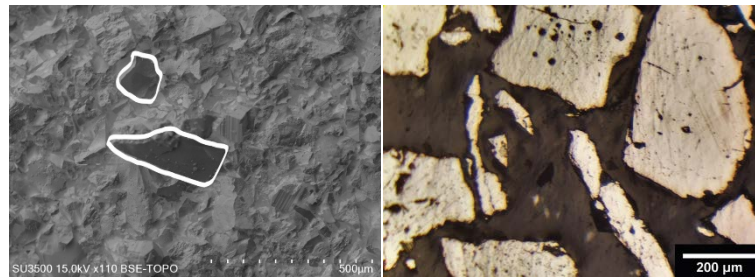


Figure 6.7 Left - SEM image of pyrite exposed to microwave radiation for 30s at a power level of 3 kW. Right - Optical microscope image of the cross section of pyrite grains after exposure to microwave radiation for 30s at a power level of 3 kW

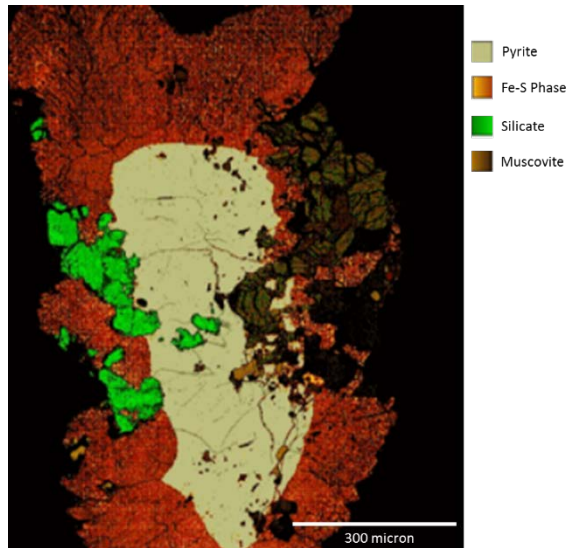


Figure 6.8 SEM image of a partial decomposition of a pyrite grain after ore was exposed to microwave radiation (Vorster, 2001)

Figure 6.9 shows an SEM image with EDS of pyrite treated for 10s in a 3 kW microwave oven. The surface does not seem to have gone through any phase changes; however, when looking at the surface phase compositions, it can be seen that oxidation has taken place. There are three different Fe-S phases of 75%, 11%, and 10%. There is also a 4% SFeO phase.

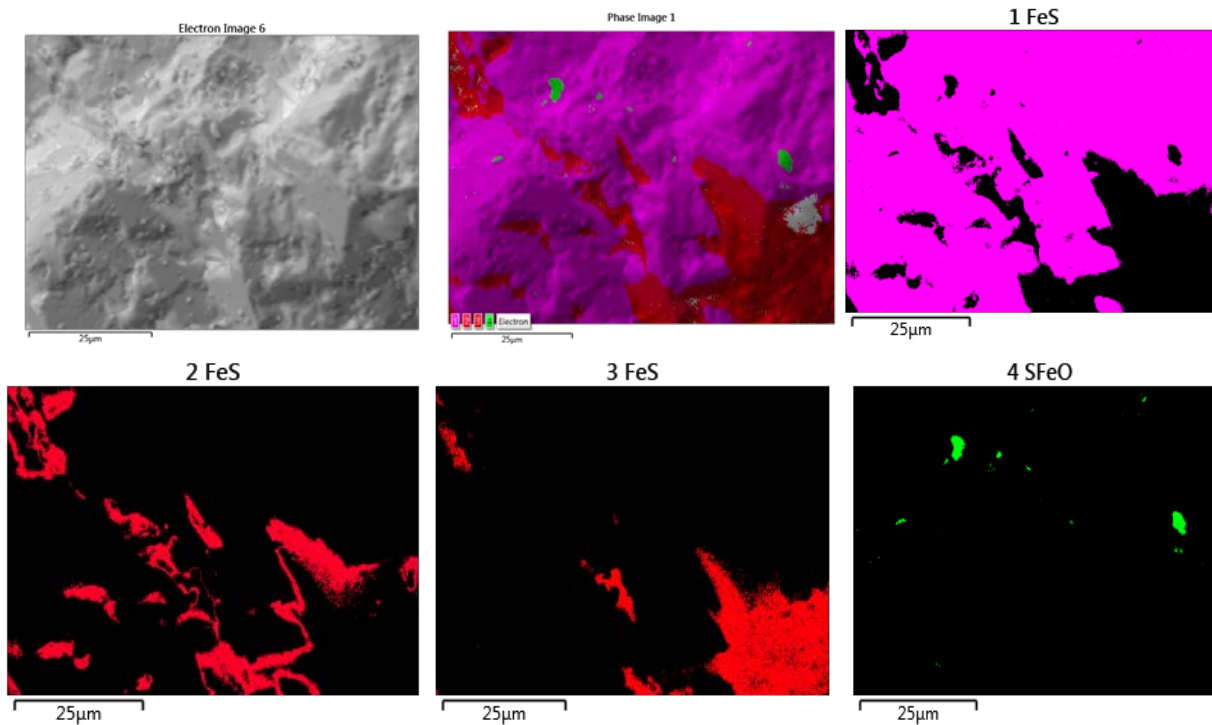


Figure 6.9 SEM image with EDS with the phase maps of a pyrite sample exposed to microwave radiation for 10s at a power level of 3 kW

6.3 Magnetic Properties

The magnetization was investigated for 3 different particle size ranges: $-425+212 \mu\text{m}$, $-212+75 \mu\text{m}$, and $-75+38 \mu\text{m}$. The treated sample was exposed to a 3kW microwave oven for 10s.

The untreated pyrite has a positive linear trend for all particle size ranges. This is characteristic of a paramagnetic mineral. The maximum magnetic susceptibility for untreated pyrite was 1×10^{-5} which occurs for the coarsest particle size range. The curves for the untreated pyrite show slight hysteresis; however, the hysteresis is not significant but it indicates a degree of ferromagnetism in the sample. Pyrite has been reported as a diamagnetic or weakly paramagnetic mineral (Ramaseshan, 1947; Rowson and Rice, 1990). This in agreement with the magnetisation results shown in Figure 6.10-Figure 6.12; which show a weakly paramagnetic trend for the untreated pyrite samples.

After exposure to microwave radiation, the magnetization curve for pyrite is similar to that of a ferromagnetic material with a saturation of magnetization at 0.2 kA/m regardless of particle size range as seen in Figure 6.10-Figure 6.12. The magnetic susceptibility of the paramagnetic component was of the treated pyrite with the particle size range of -425+212 μm is 7×10^{-5} , for the particle size range of -212+75 μm is 6×10^{-5} , and for the particle size range of -75+38 μm is 5×10^{-5} . This is in agreement with the range of magnetic susceptibility of pyrite, $3.5 \times 10^{-5} \leq \chi \leq 500 \times 10^{-5}$ (Hunt et al., 1995). Table 6.1 shows the ratio of ferromagnetic components of the treated pyrite using literature values for the saturation magnetization (Hunt et al., 1995). The increase in magnetization of the treated pyrite would suggest that magnetic separation could be a viable option for separating pyrite from other paramagnetic valuable minerals.

Table 6-1: Untreated and treated pyrite ferromagnetic components using literature data

Material	Saturation Magnetisation (kA/m)	Untreated Pyrite	Treated Pyrite	Untreated Pyrite	Treated Pyrite	Untreated Pyrite	Treated Pyrite
		(-425+212)	(-425+212)	(-212+75)	(-212+75)	(-75+38)	(-75+38)
Iron	1710	0	0.01	0	0.01	0	0.01
Hematite	2.1	1.26	5.17	0.95	5.63	0	7.22
Magnetite	471	0.01	0.02	0	0.03	0	0.03
Maghemite	367.5	0.01	0.03	0.01	0.03	0	0.04
Pyrrhotite	92.4	0.03	0.12	0.02	0.13	0	0.16

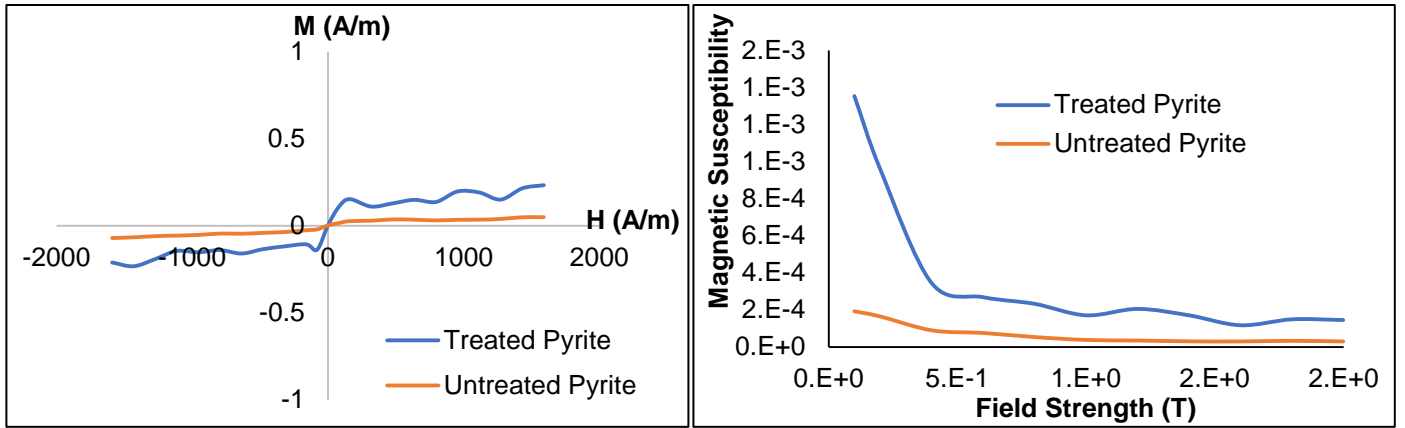


Figure 6.10 VSM results for $-425+212 \mu\text{m}$ pyrite exposed to microwave radiation for 10s at a 3kW power level.

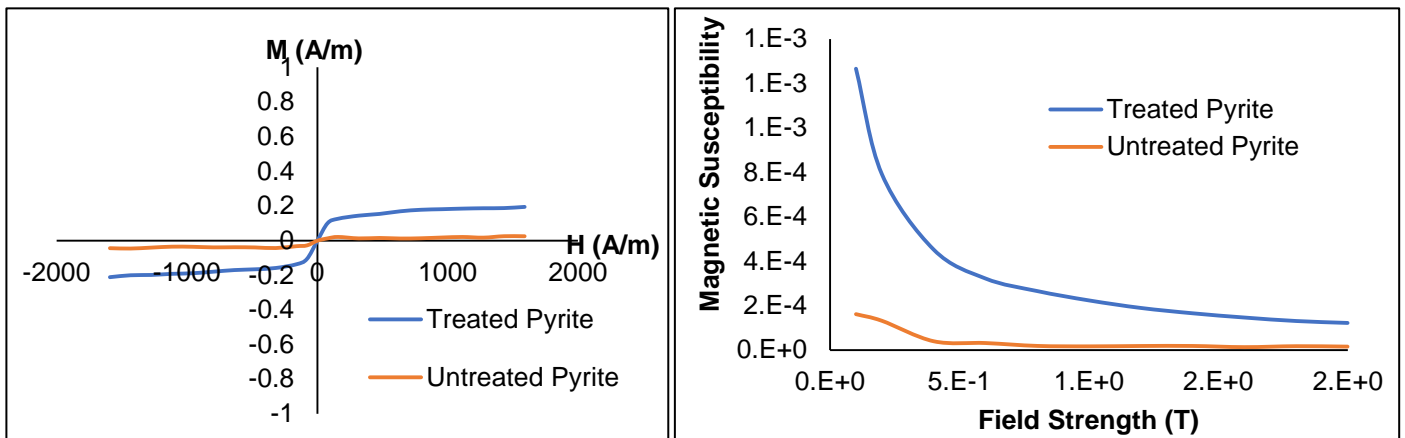
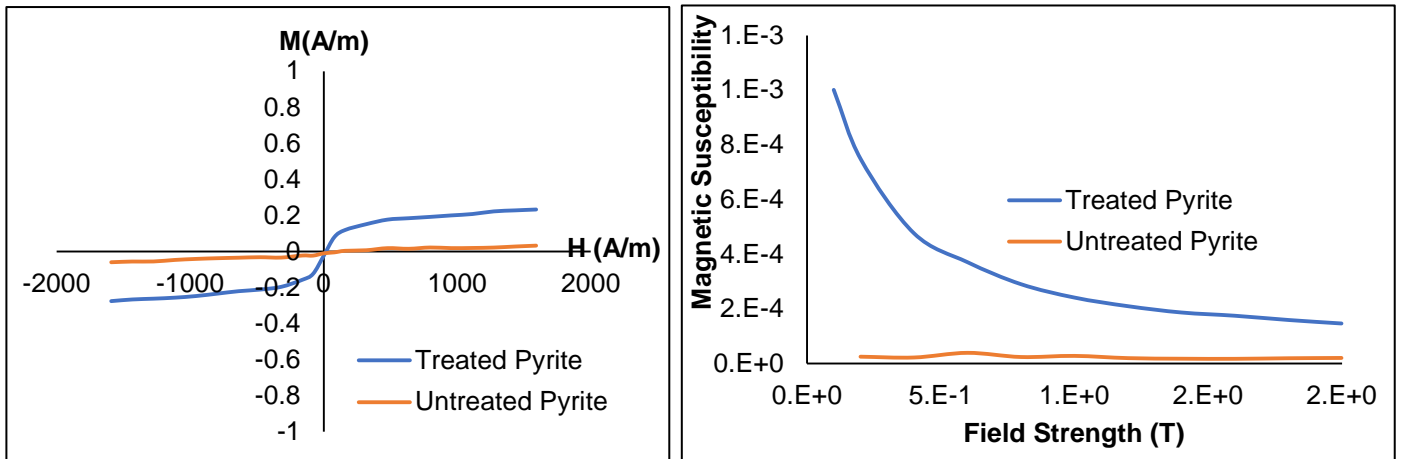


Figure 6.12 VSM results for $-75+38 \mu\text{m}$ pyrite sample exposed to microwave radiation for 10s at 3kW power level

6.4 Zeta Potential

Zeta potential measurements have been used to study the interaction of untreated pyrite and treated pyrite at pH 3 to 11 in the presence and absence of a sulfide collector.

Figure 6.13 shows the surface charge of untreated pyrite and pyrite treated for 15 and 30 s without the use of a collector. As can be seen, untreated pyrite displays a negative zeta potential at all pH values. There is a shift in the zeta potential curve to a more positive value after the microwave treatment at the lower pH values. It can also be seen that at acidic pH, the zeta potential is positive for the pyrite exposed to microwave radiation for 30s and it becomes negative at a more basic pH measurement. The zeta potential of non-oxidized sulfide minerals is negative and is comparable to sulfide minerals with a sulfur rich surface (Fornasiero et al., 1992; Fullston et al., 1999). The IEP of non-oxidised sulfide minerals such as pyrite, sphalerite, chalcopyrite and galena is similar to that of elemental sulfur and has been found at pH values between 1 and 2 (Chander, 1991; Fornasiero et al., 1994; Healy and Moignard, 1976). From the general trend observed for zeta potential changes with pH it can be concluded that the mineral surface for untreated pyrite is covered with sulfur bearing species which became positively charged through oxidation and react similarly to metal oxides (Ralston, 1991).

Upon oxidation (after pyrite has been exposed to microwave radiation) the mineral surface becomes increasingly covered with metal oxide/hydroxide species and the zeta potential versus pH curves become less negative and even positive in the case of pyrite exposed for 30s, which is consistent with literature for sulfide minerals (Fairthorne et al., 1997; King, 1982; Witika and Dobias, 1993). The IEP value is a good indication of the extent of the surface that is covered with metal oxide or hydroxide species from surface oxidation; for instance, a low IEP value indicates that the surface is lightly oxidized and an IEP value close to the corresponding metal

oxide/hydroxide indicates that the surface is heavily oxidized (Healy and Moignard, 1976). A sign reversal of zeta potential is observed for pyrite treated for 30s in a 3 kW microwave with an IEP value of 7.9 which is close to the IEP of iron oxides which range from a pH of 6.0-8.3 (Parks, 1965). This indicates that the surface of the pyrite exposed for 30s to microwave radiation is heavily oxidised.

The zeta potential measurements of pyrite after conditioning with potassium amyl xanthate (PAX) is shown in Figure 6.14. It can be seen that adsorption of PAX further decreases the charge on the surface of pyrite. This is because PAX is an anionic collector so the negatively charged xanthate ions are attracted to the positively charged surface at in the acidic pH range. The adsorption of xanthate on most sulfide minerals is an electrochemical mechanism involving chemisorption, ion exchange or oxidation. This electrochemical mechanism occurs specially in reducing or slightly oxidising conditions. This is because the oxidized surface delay or prevent the electron transfer across the mineral-solution interface (Monte et al., 2002). The ferric and ferrous ions from the oxidation products are also involved in the reaction of xanthate adsorption on the pyrite surface (Jiang et al., 1998). It has been reported that even a modest degree of oxidation of pyrite surface will produce a pyrite surface that behaves like an iron oxide (Fuerstenau et al., 1988; Woods and Richardson, 1992). The addition of PAX causes the zeta potential to become more negative in the whole pH range where no point of zero charge is observed. Similar behaviour has been reported by Fuerstenau, Mishra, and Cases (Cases et al., 1990; Jiang et al., 1998; Wang and Forssberg, 1991).

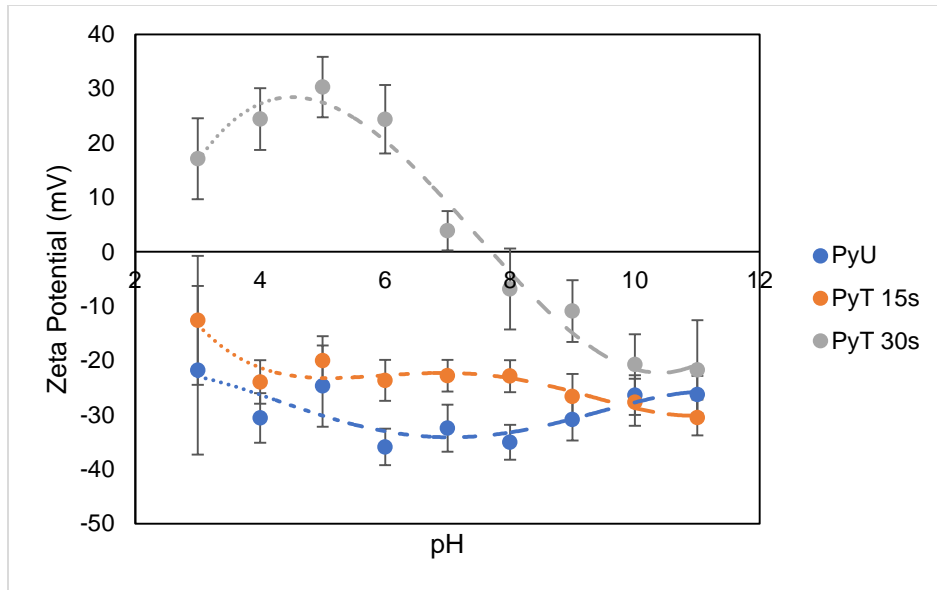


Figure 6.13 Zeta potential of collectorless untreated pyrite and pyrite treated in a 3 kW microwave oven for 15s and 30s with a 95% confidence interval.

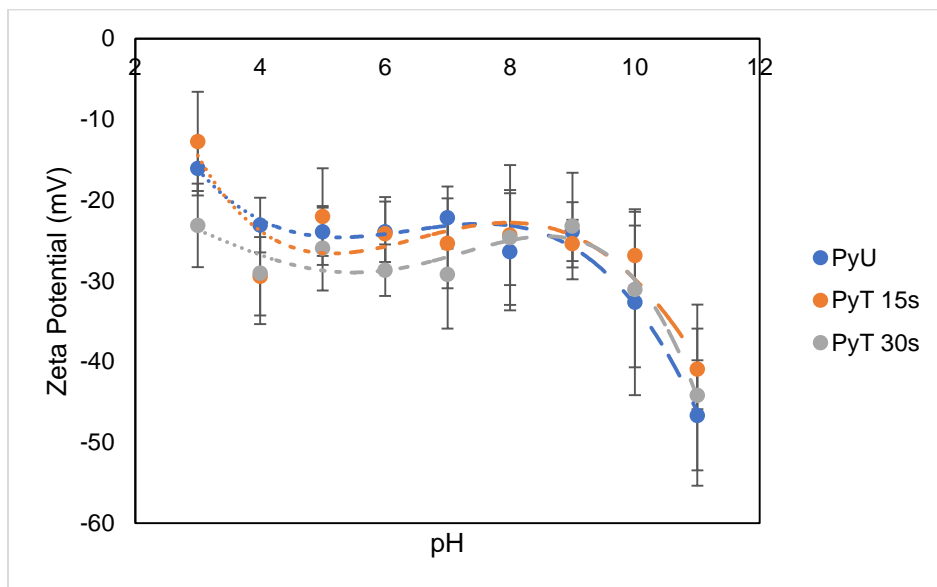


Figure 6.14 Zeta potential using PAX as a collector of untreated pyrite and pyrite treated in a 3 kW microwave oven for 15s and 30s with a 95% confidence interval.

6.5 Microflotation

The hydrophobicity and floatability of pyrite were tested through microflotation using a modified Hallimond tube. The concentration of collector addition was determined from literature (Dimou,

1986). Concentrations of 0 M, 10^{-5} M, and 10^{-4} M were tested as shown in Figure 6.16. The greatest recovery was achieved from the 10^{-4} M addition of PAX. Therefore, that concentration was used to conduct the microflotation tests.

Four condition times were also tested: 0, 5, 10, and 15 min as shown in Figure 6.15. Since condition times of 5, 10, and 15 min yielded approximately the same recovery, a conditioning time of 5 min was used to conduct all the microflotation tests.

To examine the effect of microwave radiation exposure on pyrite recovery, flotation in the absence of collector was conducted. Since pyrite is a hydrophilic mineral, no recovery is expected as seen in Figure 6.17. The flotation of pyrite is dependent on the ions present in the pulp and the pH of the system. An increase in recovery is observed in the acidic pH after exposure to microwave radiation with the greatest recovery for pyrite that was exposed for 30s at pH 3. However, this recovery is not significant as the it is only an increase of $6\pm 2\%$. There are no changes in recovery observed from pH 5-11 for treated and untreated pyrite. This is because the charge on the surface of treated pyrite has changed from being positive for acidic pH and negative for alkaline pH as can be seen in the zeta potential results in Figure 6.13; this is also consistent with literature (Naklicki et al., 2002).

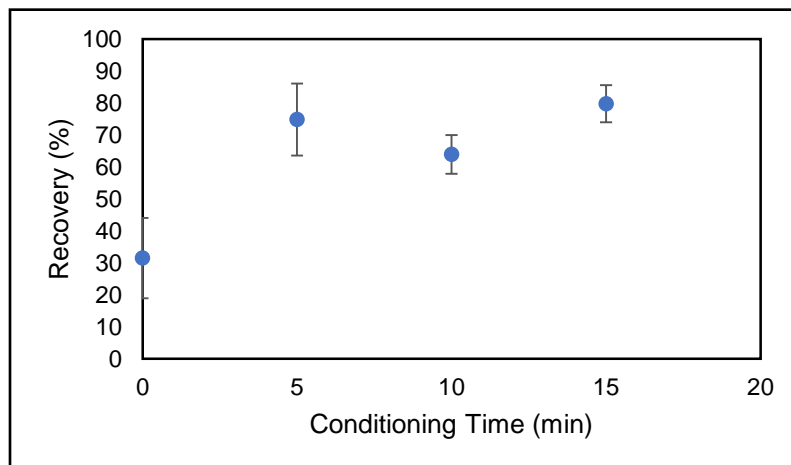


Figure 6.15 Pyrite recovery as a function of conditioning time with a 95% confidence interval

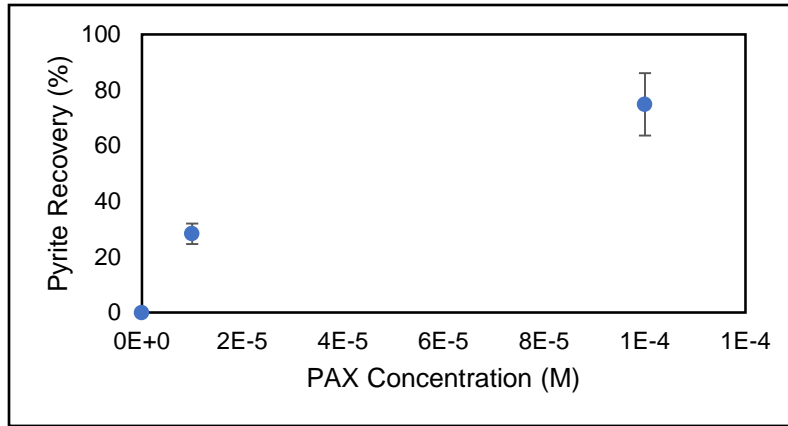


Figure 6.16 Pyrite recovery as function of PAX concentration with a 95% confidence interval

The addition of a sulfide collector, such as PAX, is often required to float sulfide minerals that are hydrophilic. As can be seen in Figure 6.18, the addition of PAX improved flotation recovery at all pH which is expected because PAX is an anionic collector which adsorbs onto the sulfur rich surface and renders the surface hydrophobic enabling the particles to attach to the air bubbles and rise. This is the reason the greatest recovery was observed for the untreated sample. Oxidized minerals can form hydroxylated surfaces when in contact with water (Fuerstenau and Pradip, 2005). Exposure to microwave radiation decreased the recovery of pyrite because PAX adsorbs onto the sulfide faces which decrease due to surface oxidation.

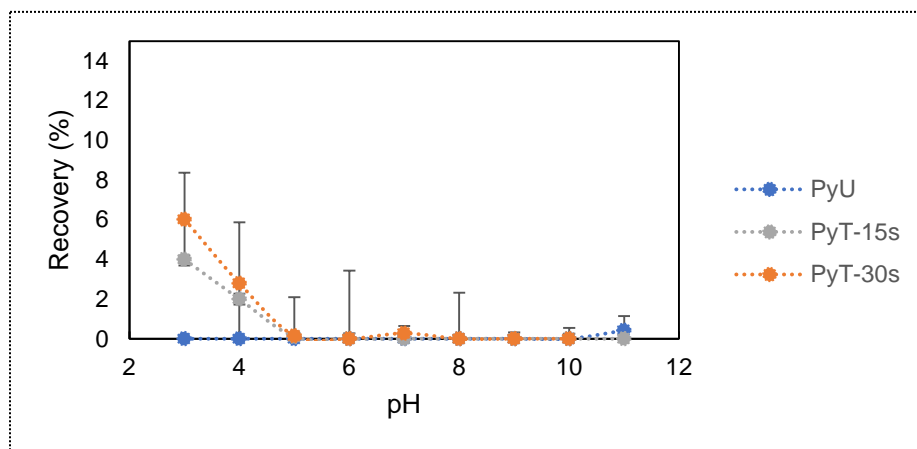


Figure 6.17 Flotation recovery without collector for untreated pyrite and pyrite treated for 15s and 30s in a 3kW microwave as a function of pH with a 95% confidence interval

At pH 11, there is no recovery. Pyrite is a gangue mineral that should be depressed during most flotation process. This can be done at pH 11. However, to make a solution very alkaline, a large amount of reagent is required. This is in agreement with literature, where Gaudin observed that an important feature in pyrite flotation was that at very alkaline pH pyrite underwent extreme depression (Gaudin, 1939). This is due to oxidation at the surface of pyrite which leads to a drastic reduction in floatability (Dimou, 1986; Glembotskii et al., 1972).

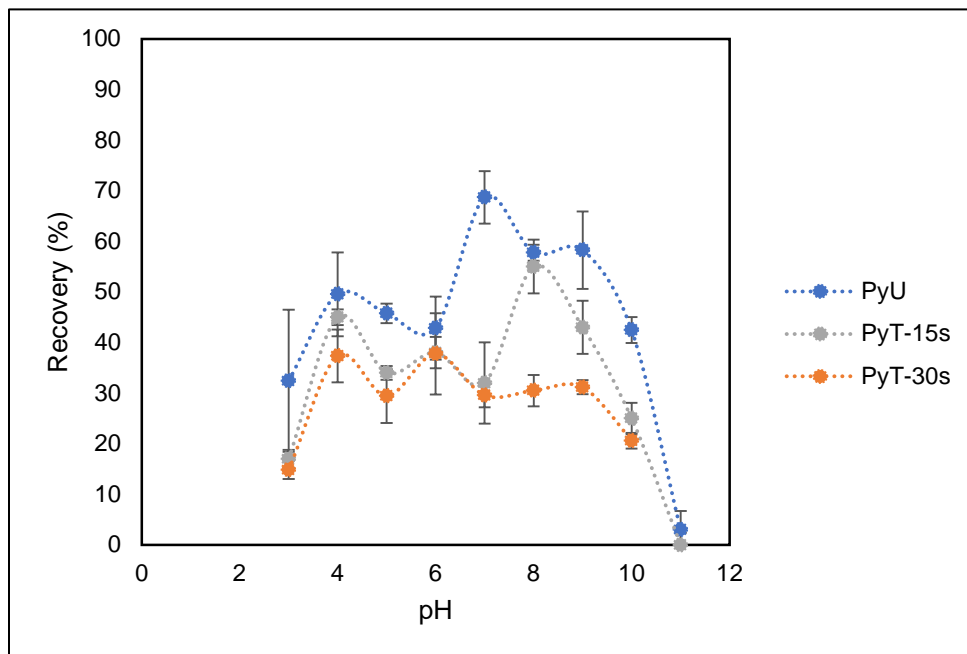


Figure 6.18 Flotation recovery with PAX for untreated pyrite and pyrite treated for 15s and 30s in a 3kW microwave as a function of pH with a 95% confidence interval

7 Conclusions and Future Work

7.1 Conclusions

The conclusions that have been determined from this work are as follows:

- The bulk temperature of pyrite was independent of particle size range. The power level and exposure time did affect the microwave heating of the pyrite sample. Increase in power level and/or increase in exposure time led to an increase in the bulk temperature of the sample.
- XRD analysis did not show any change in the peak locations to definitively conclude that phase change in the form or oxidation occurred at the surface of pyrite. XPS analysis was conducted to analyze the surface chemistry of the treated pyrite. It showed that there was formation of oxidized sulfur, sulfoxy species, ferric oxide, hydroxide, and sulfate. SEM was used to obtain surface topography and phase composition of the treated pyrite. It showed the presence of more than one Fe-S phase and SFeO phase. Thus, surface characterization of pyrite showed that phase transformation had taken place in the form of oxidation on the pyrite surface.
- Vibrating sample magnetometer (VSM) results indicated the untreated pyrite was weakly paramagnetic. After exposure to microwave radiation, pyrite became ferromagnetic. Consequently, the magnetic susceptibility of pyrite increased after exposure to microwave radiation. This is attributed to the formation of new phases which have a greater degree of magnetization. Since the treated pyrite sample is now ferromagnetic, magnetic separation can be used to remove pyrite.

- The untreated pyrite had a negative charge throughout the pH range. After microwave treatment, the charge shifted more positively. This positive shift in the zeta potential curve for treated pyrite indicates a change in the surface charge of pyrite and the presence of oxidation.
- There was an increase in the hydrophobicity of pyrite in the acid pH range after treatment. This led to an increase in pyrite recovery without the use of collector in the acidic region. A decrease in recovery of pyrite in the presence of PAX as a collector was observed after exposure to microwave radiation. This is attributed to oxidization of the pyrite surface. Hydrophilic phases were formed which inhibit the flotation process.

Previous research demonstrated the benefits of microwave pre-treatment on the comminution process. But it can also be seen that it could be beneficial for magnetic separation and froth flotation. Since the microwave treated pyrite had a lower flotation recovery, it could be a more economical option to depress pyrite.

7.2 Future work

The following are suggestions for future work:

- Since the pyrite surface has undergone oxidation, investigate the floatability of treated pyrite after conditioning with an oxide collector to understand whether this would increase the floatability of the treated pyrite.
- Study the surface properties of the product of flotation using PAX (sulfide collector) and with an oxide collector.
- Conduct magnetic separation of microwave treated sulfide ores.

- Investigate the effect of microwave radiation on the surface energetics of pyrite.
- Conduct flotation experiments on sulfide ores to see if the same conclusions are reached.

8 References

Principles of Mineral Processing. 2003, Society of Mining, Metallurgy, and Exploration, Inc., Colorado, USA.

Ahmed, N., Jameson, G.J., Flotation kinetics. *Mineral Processing and Extractive Metallurgy Review*, 1989, **5(1-4)**, 77-99.

Al-Harashsheh, M., Kingman, S., Saeid, A., Robinson, J., Dimitrakis, G., Alnawafleh, H., Dielectric properties of Jordanian oil shales. *Fuel Processing Technology*, 2009, **90(10)**, 1259-1264.

Al-Harashsheh, M., Kingman, S.W., Microwave-assisted leaching—a review. *Hydrometallurgy*, 2004, **73(3-4)**, 189-203.

Amankwah, R.K., Ofori-Sarpong, G., Microwave heating of gold ores for enhanced grindability and cyanide amenability. *Minerals Engineering*, 2011, **24(6)**, 541-544.

Andres, U., Development and prospects of mineral liberation by electrical pulses. *International Journal of Mineral Processing*, 2010, **97(1-4)**, 31-38.

Andres, U.T., Liberation study of apatite-nepheline ore comminuted by penetrating electrical discharges. *International Journal of Mineral Processing*, 1977, **4(1)**, 33-38.

Andriese, M.D., Hwang, J.Y., Bell, W., Peng, Z., Upadhyaya, A., Borkar, S.A., 2011. Microwave assisted breakage of metallic sulfide bearing ore, In *2nd International Symposium on High-Temperature Metallurgical Processing - Held During the TMS 2011 Annual Meeting and Exhibition, February 27, 2011 - March 3, 2011*. Minerals, Metals and Materials Society, San Diego, CA, United states, pp. 379-386.

Anon, 1980. Laboratory separator modification improves recovery of coarse grained heavy minerals, In *Min. Mag.*, pp. 158-161.

Anwar, J., Shafique, U., Waheed, Z., Rehman, R., Salman, M., Dar, A., Anzano, J.M., Ashraf, U., Ashraf, S., Microwave chemistry: Effect of ions on dielectric heating in microwave ovens. *Arabian J. Chem.*, 2015, **8(1)**, 100-104.

Atwater, J.E., Wheeler, R.R., Temperature dependent complex permittivities of graphitized carbon blacks at microwave frequencies between 0.2 and 26 GHz. *Journal of Materials Science*, 2004, **39(1)**, 151-157.

Ball, B., Rickard, R.S., Chemistry of Pyrite Flotation and Depression. Flotation--A. M. Gaudin Memorial, 1976.

Barani, K., Koleini, S.M.J., Rezaei, B., Magnetic properties of an iron ore sample after microwave heating. *Separation and Purification Technology*, 2011, **76(3)**, 331-336.

Bluhm, D., Fanslow, G., Nelson, S.O., Enhanced magnetic separation of pyrite from coal after microwave heating. *Magnetics, IEEE Transactions on*, 1986, **22(6)**, 1887-1890.

Bonometti, 1998. Synthesis of mixed oxides assisted by microwave heating, In *Innovations in Mineral and Coal Processing : Proceedings of the 7th International Mineral Processing Symposium*.

Böttcher, C.J.F., van Belle, O.C., Bordewijk, P., Rip, A., Yue, D.D., Theory of Electric Polarization. *J. Electrochem. Soc.*, 1974, **121(6)**, 211C.

Boulton, A., Fornasiero, D., Ralston, J., Characterisation of sphalerite and pyrite flotation samples by XPS and ToF-SIMS. *International journal of mineral processing*, 2003, **70(1)**, 205-219.

Bulatovic, S.M., *Handbook of Flotation Reagents: Chemistry, Theory and Practice: Volume 2: Flotation of Gold, PGM and Oxide Minerals*. 2010, Elsevier.

Cases, J.M., Kongolo, M., De Donato, P., Michot, L., Erre, R., Interaction between finely ground galena and pyrite with potassium amylxanthate in relation to flotation, 2. Influence of grinding media at natural pH. *International Journal of Mineral Processing*, 1990, **30(1-2)**, 35-67.

Chanaa, M.B., Lallemand, M., Mokhlisse, A., Pyrolysis of Timahdit, Morocco, oil shales under microwave field. *Fuel*, 1994, **73(10)**, 1643-1649.

Chander, S., Electrochemistry of sulfide flotation: Growth characteristics of surface coatings and their properties, with special reference to chalcopyrite and pyrite. *International Journal of Mineral Processing*, 1991, **33(1)**, 121-134.

Chatterjee, I., Misra, M., Electromagnetic and thermal modeling of microwave drying of fine coal. *Minerals and Metallurgical Processing*, 1991, **8(2)**, 110-114.

Chen, T.T., Dutrizac, J.E., Haque, K.E., Wyslouzil, W., Kashyap, S., The Relative Transparency of Minerals to Microwave Radiation. *Can. Metall. Q.*, 1984, **23(3)**, 349-351.

Cheng, J., Zhou, J., Liu, J., Cao, X., Zhou, Z., Huang, Z., Zhao, X., Cen, K., Physicochemical properties of Chinese pulverized coal ash in relation to sulfur retention. *Powder Technology*, 2004, **146(3)**, 169-175.

Chunpeng, L., 1993. The Physicochemical Properties of Nickel Bearing Pyrrhotite and Kinetics of Elemental Sulfur Produced Under Controlled Oxygen Potential in the Microwave Field, In *Extraction & Processing Division Congress*. The Minerals, Metals & Materials Society, p. 12.

Church, R.H., Webb, W.E., Salsman, J.B., 1988. Dielectric properties of low-loss minerals, In *Report of Investigations 9194*. US Department of the Interior, pp. 1-23.

Collin, R.E., *Foundation for microwave engineering*. 1966, MacGraw-Hill, Auckland [etc.].

Cumbane, A.J., 2003. Microwave treatment of minerals and ores. University of Nottingham, U.K.

Deng, M., Karpuzov, D., Liu, Q., Xu, Z., Cryo-XPS study of xanthate adsorption on pyrite. *Surf. Interface Anal.*, 2013, **45(4)**, 805-810.

Dimou, A., 1986. The flotation of pyrite using xanthate collectors, In *Chemical Engineering*. University of Cape Town, Cape Town, South Africa.

Eskibalci, M.F., Ozkan, S.G., An investigation of effect of microwave energy on electrostatic separation of colemanite and ulexite. *Minerals Engineering*, 2012, **31(0)**, 90-97.

Fairthorne, G., Fornasiero, D., Ralston, J., Effect of oxidation on the collectorless flotation of chalcopyrite. *International Journal of Mineral Processing*, 1997, **49(1-2)**, 31-48.

Fan, X., Rowson, N.A., Fundamental investigation of microwave pretreatment on the flotation of massive ilmenite ores. *Developments in Chemical Engineering and Mineral Processing*, 2000, **8(1)**, 167-182.

Fan, X., Rowson, N.A., 2002. Surface modification and column flotation of a massive ilmenite ore, 2 ed. Metallurgical Society of CIM, pp. 133-142.

Fandrich, R., Gu, Y., Burrows, D., Moeller, K., Modern SEM-based mineral liberation analysis. *International Journal of Mineral Processing*, 2007, **84(1-4)**, 310-320.

Feteris, S.M., Frew, J.A., Jowett, A., Modelling the effect of froth depth in flotation. *International Journal of Mineral Processing*, 1987, **20(1-2)**, 121-135.

Fitzgibbon, K.E., Veasey, T.J., Thermally assisted liberation - a review. *Minerals Engineering*, 1990, **3(1-2)**, 181-185.

Foner, S., Vibrating sample magnetometer. *Rev. Sci. Instrum.*, 1956, **27(7)**, 548-548.

Fornasiero, D., Eijt, V., Ralston, J., An electrokinetic study of pyrite oxidation. *Colloids and Surfaces*, 1992, **62(1)**, 63-73.

Fornasiero, D., Li, F., Ralston, J., Oxidation of Galena. *Journal of Colloid and Interface Science*, 1994, **164(2)**, 345-354.

Fuerstenau, D.W., Activation in the flotation of sulfide minerals. *South African Institute of Mining and Metallurgy, Principles of Flotation*, 1982, 183-198.

Fuerstenau, D.W., Abouzeid, A.Z.M., The energy efficiency of ball milling in comminution. *International Journal of Mineral Processing*, 2002, **67(1-4)**, 161-185.

Fuerstenau, D.W., Pradip, Zeta potentials in the flotation of oxide and silicate minerals. *Adv. Colloid Interface Sci.*, 2005, **114-115**, 9-26.

Fuerstenau, M.C., Kuhn, M.C., Elgillani, D.A., The role of dixanthogen in xanthate flotation of pyrite. *Trans. AIME*, 1968, **241**, 148-156.

Fuerstenau, M.C., Lopez-Valdivieso, A., Fuerstenau, D.W., Role of hydrolyzed cations in the natural hydrophobicity of talc. *International Journal of Mineral Processing*, 1988, **23(3-4)**, 161-170.

Fullston, D., Fornasiero, D., Ralston, J., Zeta potential study of the oxidation of copper sulfide minerals. *Colloids and Surfaces A: Physicochemical and Engineering Aspects*, 1999, **146(1-3)**, 113-121.

Gaete-Garretón, L.F., Vargas-Hermández, Y.P., Velasquez-Lambert, C., Application of ultrasound in comminution. *Ultrasonics*, 2000, **38(1-8)**, 345-352.

Gaudin, A.M., *Principles of mineral dressing*. 1939, McGraw-Hill Book Company, Inc., New York; London.

Gaudin, A.M., De Bruyn, P.L., Mellgren, O., Adsorption of ethyl xanthate on pyrite. *Mining Eng. Jan*, 1956, 65-70.

Glembotskii, V.A., Klassen, V.I., Plaksin, I.N., 1972. The effect of mineral particle size on flotation. *Flotation*.

Granville, A., Allison, S.A., Finkelstein, N.P., 1972. A review of reactions in the flotation system galena-xanthate-oxygen. Mintek.

Güngör, A., Atalay, Ü., 1998. Microwave Processing and Grindability, In *7th International Mineral Processing Symposium*, pp. 13-17.

Hall, D.A., Ben-Omran, M.M., Stevenson, P.J., Field and temperature dependence of dielectric properties in BaTiO₃-based piezoceramics. *Physics: Condensed Matter*, 1998, **10**, 461-476.

Haque, K.E., Microwave energy for mineral treatment processes—a brief review. *International Journal of Mineral Processing*, 1999, **57(1)**, 1-24.

Harris, P.J., Influence of the substituent group on the decomposition of xanthates in aqueous solutions. *S. Afr. J. Chem.*, 1984, **37(3)**, 91-95.

He, S., Fornasiero, D., Skinner, W., Correlation between copper-activated pyrite flotation and surface species: Effect of pulp oxidation potential. *Minerals Engineering*, 2005, **18(12)**, 1208-1213.

Healy, T.W., Moignard, M.S., A review of electrokinetic studies of metal sulphides. *Flotation*, 1976, **1**, 275-297.

Henda, R., Hermas, A., Gedye, R., Islam, M.R., Microwave enhanced recovery of nickel-copper ore: communitation and floatability aspects. *Journal of Microwave Power and Electromagnetic Energy*, 2005, **40(1)**, 7-16.

Hunt, C.P., Moskowitz, B.M., Banerjee, S.K., Magnetic properties of rocks and minerals. *Rock physics & phase relations: a handbook of physical constants*, 1995, 189-204.

Hunter, R.J., Recent developments in the electroacoustic characterisation of colloidal suspensions and emulsions. *Colloids and Surfaces A: Physicochemical and Engineering Aspects*, 1998, **141(1)**, 37-66.

Irannajad, M., Mehdilo, A., Salmani Nuri, O., Influence of microwave irradiation on ilmenite flotation behavior in the presence of different gangue minerals. *Separation and Purification Technology*, 2014, **132**, 401-412.

Jiang, C.L., Wang, X.H., Parekh, B.K., Leonard, J.W., The surface and solution chemistry of pyrite flotation with xanthate in the presence of iron ions. *Colloids and Surfaces A: Physicochemical and Engineering Aspects*, 1998, **136(1)**, 51-62.

Jordens, A., 2016. The beneficiation of rare earth element bearing minerals, In *Mining and Materials Engineering*. McGill University, Montreal, Canada.

Jordens, A., Marion, C., Kuzmina, O., Waters, K.E., Physicochemical aspects of allanite flotation. *J. Rare Earths*, 2014a, **32(5)**, 476-486.

Jordens, A., Marion, C., Kuzmina, O., Waters, K.E., Surface chemistry considerations in the flotation of bastnäsite. *Minerals Engineering*, 2014b, **66-68**, 119-129.

Kappe, C.O., Stadler, A., Dallinger, D., *Microwaves in organic and medicinal chemistry*. 2012.

Kelly, E.G., Spottiswood, D.J., The theory of electrostatic separations: A review Part I. Fundamentals. *Minerals Engineering*, 1989a, **2(1)**, 33-46.

Kelly, E.G., Spottiswood, D.J., The theory of electrostatic separations: A review part III. The separation of particles. *Minerals Engineering*, 1989b, **2(3)**, 337-349.

Kelly, R.M., Rowson, N.A., Microwave reduction of oxidised ilmenite concentrates. *Minerals Engineering*, 1995, **8(11)**, 1427-1438.

King, R.P., *Principles of flotation*. South African Institute of Mining and Metallurgy, Kelvin House, 2 Holland St, Johannesburg, South Africa, 1982. 268, 1982.

King, R.P., Schneider, C.L., Mineral liberation and the batch comminution equation. *Minerals engineering*, 1998, **11(12)**, 1143-1160.

Kingman, S.W., Jackson, K., Cumbane, A., Bradshaw, S.M., Rowson, N., Greenwood, R., Recent developments in microwave assisted comminution. *International Journal of Mineral Processing*, 2004, **74**, 71-83.

Kingman, S.W., Rowson, N.A., Microwave treatment of minerals-a review. *Minerals Engineering*, 1998, **11(11)**, 1081-1087.

Kingman, S.W., Vorster, W., Rowson, N.A., The influence of mineralogy on microwave assisted grinding. *Minerals Engineering*, 2000, **13(3)**, 313-327.

Kingston, H.M., Jassie, L.B., Introduction to Microwave Sample Preparation: Theory and Practice. *Anal. Chem.*, 1989, **61(5)**, 330A-330A.

Kobusheshe, J., 2010. Microwave enhanced processing of ores. University of Nottingham.

Koleini, S.M.J., Barani, K., *Microwave Heating Applications in Mineral Processing*. 2012.

Krishnan, K.H., Mohanty, D.B., Sharma, K.D., The effect of microwave irradiations on the leaching of zinc from bulk sulphide concentrates produced from Rampura-Agucha tailings. *Hydrometallurgy*, 2007, **89(3-4)**, 332-336.

Laajalehto, K., Leppinen, J., Kartio, I., Laiho, T., XPS and FTIR study of the influence of electrode potential on activation of pyrite by copper or lead. *Colloids and Surfaces A: Physicochemical and Engineering Aspects*, 1999, **154(1-2)**, 193-199.

Leonelli, C., Mason, T.J., Microwave and ultrasonic processing: Now a realistic option for industry. *Chemical Engineering and Processing: Process Intensification*, 2010, **49(9)**, 885-900.

Lovás, M., Murová, I., Mockovciaková, A., Rowson, N., Jakabský, Š., Intensification of magnetic separation and leaching of Cu-ores by microwave radiation. *Separation and Purification Technology*, 2003, **31(3)**, 291-299.

Majima, H., *Electrochemistry of pyrite and its significance in sulphide flotation*. 1971.

Marion, C., Jordens, A., McCarthy, S., Grammatikopoulos, T., Waters, K.E., An investigation into the flotation of muscovite with an amine collector and calcium lignin sulfonate depressant. *Separation and Purification Technology*, 2015, **149**, 216-227.

Marland, S., Han, B., Merchant, A., Rowson, N., The effect of microwave radiation on coal grindability. *Fuel*, 2000, **79(11)**, 1283-1288.

Marland, S., Merchant, A., Rowson, N., Dielectric properties of coal. *Fuel*, 2001, **80(13)**, 1839-1849.

Meredith, R.J., 1998. Microwave interaction with dielectric materials, In *Engineers' Handbook of Industrial Microwave Heating*, ed. Warne, A.T.J.a.D.F. Institution of Electrical Engineers, London, UK, pp. 19-52.

Metaxas, A.C., *Foundations of electroheat : a unified approach*. 1996, Wiley, Chichester; New York.

Metaxas, A.C., Meredith, R.J., Engineers, I.o.E., 1988. *Industrial microwave heating*. P. Peregrinus on behalf of the Institution of Electrical Engineers, London, UK.

Metso, Sandgren, E., Berglinz, B., Modigh, S., *Basics in Minerals Processing Handbook*. 2015, Metso Corporation.

Minerals, M., 2004. *Basics in Mineral Processing*. Ed.

Minniberger, S., Diorico, F., Haslinger, S., Hufnagel, C., Novotny, C., Lippok, N., Majer, J., Koller, C., Schneider, S., Schmiedmayer, J., Magnetic conveyor belt transport of ultracold atoms to a superconducting atomchip. *Appl. Phys. B*, 2014, **116(4)**, 1017-1021.

Monte, M.B.M., Dutra, A.J.B., Albuquerque Jr, C.R.F., Tondo, L.A., Lins, F.F., The influence of the oxidation state of pyrite and arsenopyrite on the flotation of an auriferous sulphide ore. *Minerals Engineering*, 2002, **15(12)**, 1113-1120.

Murariu, V., Svoboda, J., The applicability of Davis Tube tests to ore separation by drum magnetic separators. *Physical Separation in Science and Engineering*, 2003, **12(1)**, 1-11.

Muzenda, E., Afolabi, A.S., Effect of oxygen and micro-cracking on the flotation of low grade nickel sulphide ore. *World Academy of Science, Engineering and Technology*, 2010, **70**, 723-728.

Nadolski, S., Klein, B., Kumar, A., Davaanyam, Z., An energy benchmarking model for mineral comminution. *Minerals Engineering*, 2014, **65**, 178-186.

Nagaraj, D.R., Ravishankar, S.A., Flotation reagents—A critical overview from an industry perspective. *Froth Flotation: A Century of Innovation*. Society for Mining, Metallurgy, and Exploration, Littleton, Colorado, 2007, 375-424.

Naklicki, M.L., Rao, S.R., Gomez, M., Finch, J.A., Flotation and surface analysis of the nickel (II) oxide/amyxanthate system. *International Journal of Mineral Processing*, 2002, **65(2)**, 73-82.

Napier-Munn, T., Is progress in energy-efficient comminution doomed? *Minerals Engineering*, 2015, **73**, 1-6.

Napier-Munn, T.J.e.a., *Mineral comminution circuits : their operation and optimisation*. 1999, Julius Kruttschnitt Mineral Research Centre, Indooroopilly, Qld.

Naveau, A., Monteil-Rivera, F., Guillon, E., Dumonceau, J., XPS and XAS studies of copper(II) sorbed onto a synthetic pyrite surface. *Journal of Colloid and Interface Science*, 2006, **303(1)**, 25-31.

Nesbitt, H.W., Bancroft, G.M., Pratt, A.R., Scaini, M.J., Sulfur and iron surface states on fractured pyrite surfaces. *Am. Mineral.*, 1998, **83(9-10)**, 1067-1076.

Nickel, E.H., The Definition of a Mineral. *The Canadian Mineralogist*, 1995, **33**, 689-690.

O'Brian, R.W., Electro-acoustic effects in a dilute suspension of spherical particles. *J. Fluid Mech.*, 1988, **190**, 71-86.

Parekh, B.K., Epstein, H.E., Goldberger, W.M., Novel comminution process uses electric and ultrasonic energy. *Min. Eng.*, 1984, **36(9)**, 1305-1309.

Parks, G.A., The isoelectric points of solid oxides, solid hydroxides, and aqueous hydroxo complex systems. *Chem. Rev.*, 1965, **65(2)**, 177-198.

Polat, M., Chander, S., First-order flotation kinetics models and methods for estimation of the true distribution of flotation rate constants. *International Journal of Mineral Processing*, 2000, **58(1)**, 145-166.

Pope, M.I., Sutton, D.I., The correlation between froth flotation response and collector adsorption from aqueous solution. Part I. Titanium dioxide and ferric oxide conditioned in oleate solutions. *Powder Technology*, 1973, **7(5)**, 271-279.

Premaratne, W.A.P.J., 2004. Mineral chemistry and metal extraction of Sri Lankan beach sand. University of Birmingham, Birmingham.

Radziszewski, P., Energy recovery potential in comminution processes. *Minerals Engineering*, 2013, **46-47**, 83-88.

Ralston, J., Eh and its consequences in sulphide mineral flotation. *Minerals Engineering*, 1991, **4(7-11)**, 859-878.

Ramaseshan, S., The magnetic properties of iron-pyrites. *Proceedings Mathematical Sciences*, 1947, **25(2)**, 201-207.

Riley, J., 2009. Charge in Colloidal Systems, In *Colloid Science*. Blackwell Publishing Ltd., pp. 14-35.

Robert, C.O., Handley, O., 2000. Modern magnetic materials: principles and applications. New York: Wiley-Interscience.

Rowson, N.A., Rice, N.M., Magnetic enhancement of pyrite by caustic microwave treatment. *Minerals Engineering*, 1990, **3(3-4)**, 355-361.

Sahyoun, C., Kingman, S.W., Rowson, N.A., The effect of heat treatment on chalcopyrite. *Physical Separation in Science and Engineering*, 2003, **12(1)**, 23-30.

Sahyoun, C., Kingman, S.W., Rowson, N.A., High powered microwave treatment of carbonate copper ore. *European Journal of Mineral Processing and Environmental Protection*, 2004, **4(3)**, 175-182.

Schiffmann, R.F., Microwave and dielectric drying. *Handbook of industrial drying*, 1995, **1**, 345-372.

Sebastian, M.T., Jantunen, H., Low loss dielectric materials for LTCC applications: a review. *Int. Mater. Rev.*, 2008, **53**, 57-90.

Sharma, A., 2016. Introduction to colloid and interface science and engineering. Indian Institute of Technology Kanpur, Madras, India.

Shi, F., Zuo, W., Manlapig, E., Characterisation of pre-weakening effect on ores by high voltage electrical pulses based on single-particle tests. *Minerals Engineering*, 2013, **50–51(0)**, 69-76.

Smith, R.D., Corporation, T.E., Institute, E.P.R., *Microwave power in industry*. 1984, Electric Power Research Institute, Palo Alto, Calif.

Standish, N., Worner, H., Microwave application in the reduction of metal oxides with carbon. *Journal of Microwave Power and Electromagnetic Energy*, 1990, **25(3)**.

Standish, N., Worner, H., Gupta, G., Temperature distribution in microwave-heated iron ore-carbon composites. *Journal of microwave power and electromagnetic energy*, 1990, **25(2)**, 75-80.

Standish, N., Worner, H.K., Obuchowski, D.Y., Particle size effect in microwave heating of granular materials. *Powder technology*, 1991, **66(3)**, 225-230.

Sutherland, K.L., Wark, I.W., 1955. Principles of flotation. Australasian Institute of Mining and Metallurgy.

Suzuki, T., Relation between Flotability and Types of Pyrite. *The Science Reports of the Tohoku Univ.*, Series III, X, 1967(**1**), 173-481.

Svoboda, J., The effect of magnetic field strenght on the efficiency of magnetic separation. *Minerals Engineering*, 1994, **7(5-6)**, 747-757.

Svoboda, J., A realistic description of the process of high-gradient magnetic separation. *Minerals Engineering*, 2001, **14(11)**, 1493-1503.

Szargan, R., Karthe, S., Suoninen, E., XPS studies of xanthate adsorption on pyrite. *Applied surface science*, 1992, **55(4)**, 227-232.

Teipel, U., Leisinger, K., Mikonsaari, I., Comminution of crystalline material by ultrasonics. *International Journal of Mineral Processing*, 2004, **74, Supplement(0)**, S183-S190.

Trefalt, G., Borkovec, M., 2014. Overview of DLVO Theory. University of Geneva, Geneva.

Uslu, T., Atalay, Ü., 2003. Microwave heating characteristics and microwave assisted magnetic enhancement of pyrite, In *International Mining Congress and Exhibition of Turkey-IMCET*.

Uslu, T., Atalay, Ü., Microwave heating of coal for enhanced magnetic removal of pyrite. *Fuel Processing Technology*, 2004, **85(1)**, 21-29.

Uslu, T., Atalay, Ü., Arol, A.I., Effect of microwave heating on magnetic separation of pyrite. *Colloids and Surfaces A: Physicochemical and Engineering Aspects*, 2003, **225(1-3)**, 161-167.

Veasey, T.J., 1986. Thermally assisted liberation of non-sulphide ore, In *1st Int. Mineral Proc. Symp.*, Izmir, Turkey, p. 557.

Veasey, T.J., Wills, B.A., Review of methods of improving mineral liberation. *Minerals Engineering*, 1991, **4(7-11)**, 747-752.

Vorster, W., 2001. The effect of microwave radiation on mineral processing. University of Birmingham.

Vorster, W., Rowson, N.A., Kingman, S.W., The effect of microwave radiation upon the processing of Neves Corvo copper ore. *International Journal of Mineral Processing*, 2001, **63(1)**, 29-44.

Walkiewicz, J.W., Kazonich, G., McGill, S.L., Microwave heating characteristics of selected minerals and compounds. *Minerals and Metallurgical Processing*, 1988, **5(1)**, 39-42.

Walkiewicz, J.W., Lindroth, D.P., Clark, A.E., Grindability of Taconite Rod Mill Feed Enhanced by Microwave-Induced Cracking. *Society of Mining Engineers of Aime*, 1993.

Walkiewicz, J.W., Raddatz, A.E., McGill, S.L., 1989. Microwave-assisted grinding, In *Industry Applications Society Annual Meeting, 1989., Conference Record of the 1989 IEEE*. IEEE, pp. 1528-1532.

Wang, E., Shi, F., Manlapig, E., Mineral liberation by high voltage pulses and conventional comminution with same specific energy levels. *Minerals Engineering*, 2012, **27–28(0)**, 28-36.

Wang, X.H., Forssberg, K.S.E., Mechanisms of pyrite flotation with xanthates. *International journal of mineral processing*, 1991, **33(1-4)**, 275-290.

Waters, K.E., 2007. The effect of thermal treatment on the physicochemical properties of minerals, In *Chemical Engineering*. University of Birmingham, Birmingham, p. 367.

Waters, K.E., Rowson, N.A., Greenwood, R.W., Williams, A.J., Characterising the effect of microwave radiation on the magnetic properties of pyrite. *Separation and Purification Technology*, 2007, **56(1)**, 9-17.

Waters, K.E., Rowson, N.A., Greenwood, R.W., Williams, A.J., The effect of heat treatment on the magnetic properties of pyrite. *Minerals Engineering*, 2008, **21(9)**, 679-682.

Watts, J.F., Wolstenholme, J., John, W., Sons, *An introduction to surface analysis by XPS and AES*. 2003, J. Wiley, Chichester, West Sussex, England; New York.

Weisener, C., Gerson, A., Cu(II) adsorption mechanism on pyrite: an XAFS and XPS study. *Surf. Interface Anal.*, 2000a, **30(1)**, 454-458.

Weisener, C., Gerson, A., An investigation of the Cu (II) adsorption mechanism on pyrite by ARXPS and SIMS. *Minerals Engineering*, 2000b, **13(13)**, 1329-1340.

Wencheng, X., Jianguo Yan, G., Experimental design of oily bubbles in oxidized coal flotation. *Gospodarka Surowcami Mineralnymi*, 2013, **29(4)**, 130-135.

Wills, B.A., Comminution in the minerals industry - An overview. *Minerals Engineering*, 1990, **3(1-2)**, 3-5.

Wills, B.A., Finch, J.A., *Wills' mineral processing technology : an introduction to the practical aspects of ore treatment and mineral recovery*. 2016.

Wills, B.A., Parker, R.H., Binns, D.G., Thermally assisted liberation of cassiterite. *Minerals and Metallurgical Processing*, 1987, **4(2)**, 94.

Witika, L.K., Dobias, B., Electrokinetics of sulphide minerals: Fundamental surface reactions of carrollite. *Minerals Engineering*, 1993, **6(8)**, 883-894.

Woods, R., Richardson, P.E., *Electrochemistry in Mineral and Metal Processing III*. St. Louis, 1992, 1992.

Wu, L.Z., Ding, J., Jiang, H.B., Chen, L.F., Ong, C.K., Particle size influence to the microwave properties of iron based magnetic particulate composites. *J. Magn. Magn. Mater.*, 2005, **285(1)**, 233-239.

Yerkovic, C., Menacho, J., Gaete, L., Exploring the ultrasonic comminution of copper ores. *Minerals Engineering*, 1993, **6(6)**, 607-617.

Znamenáčková, I., Lovás, M., Mockovčiaková, A., Jakabský, Š., Briančin, J., Modification of magnetic properties of siderite ore by microwave energy. *Separation and Purification Technology*, 2005, **43(2)**, 169-174.